Interferon Regulatory Factor-1 protects from fatal neurotropic infection with Vesicular Stomatitis Virus

Von der Fakultät für Lebenswissenschaften

der Technischen Universität Carolo-Wilhelmina zu Braunschweig

zur Erlangung des Grades einer

Doktorin der Naturwissenschaften

(Dr. rer. nat.)

genehmigte

D i s s e r t a t i o n

von Sharmila Nair

aus New Delhi, India

1. Referent: Privatdozet Dr. Gerhard Gross

2. Referent: Professor. Martin Korte

3. Referent: Professor Dr. Karl-Klaus Conzelmann

eingereicht am: 20.02.2014

mündliche Prüfung (Disputation) am:28.04.2014

Druckjahr 2014

Vorveröffentlichungen der Dissertation

Teilergebnisse aus dieser Arbeit wurden mit Genehmigung der Fakultät für Lebenswissenschaften, vertreten durch meinen Mentor der Arbeit, in folgenden Beiträgen vorab veröffentlicht:

Publikationen

Nair, S., Michaelsen-Preusse, K., Finsterbusch, K., Stegemann-Koniszewski, S. Bruder, D., Grashoff, M., Korte, M., Köster, M., Kalinke, U., Hauser,H., Kröger, A. Interferon Regulatory Factor-1 protects from fatal neurotropic infection with Vesicular Stomatitis Virus by specific inhibition of viral replication in neurons**.** PloS Pathogens 2014 (accepted)

Tagungsbeiträge

Nair, S., Kröger, A. Innate immune functions interferon regulatory factor-1 in antiviral responses (Talk). 6th International Workshop on Interferon and Infection (2013)

Nair, S., Kröger, A. Molecular mechanisms of IRF 1 dependent, anti-viral response (Talk). Autumn School of Immunology, Bad Schandau (2011).

Posterbeiträge

Nair, S., Michaelson-Preusse, K., Kröger. The Interferon Regulatory Factor-1 protects mice from lethal neuropathogenesis (poster). J6 Keystone Symposia, USA (2014)

Nair, S., Kröger, A. Innate Immune functions of Interferon Regulatory Factor-1 in antiviral responses (poster). NWG Neuroscience conference, Göttingen (2013)

Nair, S., Kröger, A. IRF-1 mediated anti-viral response against VSV (poster). Summer School, Rügen (2012)

CONTENTS

1 ABSTRACT

The innate immune system protects cells against invading viral pathogens by the auto- and paracrine action of type I interferon (IFN). In addition, the interferon regulatory factor (IRF)-1 can induce alternative intrinsic antiviral responses. Although both, type I IFN and IRF-1 mediate their antiviral action by inducing overlapping subsets of IFN stimulated genes, the functional role of this alternative antiviral action of IRF-1 in context of viral infections *in vivo* remains unknown. Here, we report that IRF-1 is essential to counteract the neuropathology of vesicular stomatitis virus (VSV). IFN- and IRF-1-dependent antiviral responses act sequentially to create a layered antiviral protection program against VSV infections. Upon intranasal infection, VSV is cleared in the presence or absence of IRF-1 in peripheral organs, but IRF-$1^{-/-}$ mice continue to propagate the virus in the brain and succumb. Although rapid IFN induction leads to a decline in VSV titres early on, viral replication is re-enforced in the brains of IRF-$1^{-/-}$ mice. While IFN provides short-term protection, IRF-1 is induced with delayed kinetics and controls viral replication at later stages of infection. IRF-1 has no influence on viral entry but inhibits viral replication in neurons and viral spread through the CNS, which leads to fatal inflammatory responses in the CNS. These data support a temporal, non-redundant antiviral function of type I IFN and IRF-1, the latter playing a crucial role in late time points of VSV infection in the brain.

2 INTRODUCTION

2.1 Viral detection and signaling

Recognition of invading pathogens is central to the host immune system. The innate immune system which is considered the first line of defences depends on a limited number of germline encoded receptors called pathogen recognition receptors (PRRs) to recognize pathogen-associated molecular patterns (PAMPs). Two families of PRRs that recognize viral nucleic acid have been characterized in detail **(listed in Table 1)**. The first is a subfamily of Toll-like receptors (TLRs) that is made up of TLR1, TLR2, TLR3, TLR7, TLR8 and TLR9, which are mainly expressed in the endosomes of some cell types. The second family of receptors comprises the retinoic-acid-inducible gene I (RIG-I)-like receptors (RLRs), encompassing RIG-I, melanoma differentiation-associated gene 5 (MDA5).

Depending on the nature of the pathogen and cell type involved, signal transduction pathways are activated by PAMP-engaged PRRs so as to elicit antimicrobial responses by inducing various target genes that include those encoding type I IFNs, proinflammatory cytokines, and chemokines. Three major signalling pathways responsible for mediating PRR responses include (i) NF-κB, (ii) mitogen-activated protein kinases (MAPKs), and (iii) IFN regulatory factors (IRFs). While NF-κB and MAPKs play central roles in induction of a proinflammatory response, IRFs are essential for stimulation of IFN production.

Table 1: Viral PAMPs

PRR	Viral PAMP	Virus (reference)
TLR3	Endosomal dsRNA	RNA viruses [1,2] such as • Reovirus [3] • MCMV [4] • Rhinovirus [5] • West Nile virus [6] • Influenza A [7]
TLR7	ssRNA	• Influenza A [8-10] • VSV [10]
TLR8	ssRNA	• HIV [8]
TLR9	Unmethylated DNA	• HSV-1/2 [11-13] • MCMV [14]
RIG-I	Cytoplasmic 5'-triphosphate dsRNA	• Flaviviruses [15,16] • Paramyxovirus such as RSV-1 [15,17] • Orthomyxovirus, for example, influenza A virus [15] and EBV [18]
MDA5	Cytoplasmic dsRNA	• Picornaviruses [15,19] such as EMCV

2.2 The IFN action

Interferons (IFNs) are a group of secreted cytokines that are known to elicit distinct antiviral effects. Discovered in 1957 by Lindenmann and Isaacs for their antiviral properties [20], the type I IFNs are now grouped into three classes called type I, II and III IFNs, according to their amino acid sequence. Type I

IFNs comprise a large group of molecules; mammals have multiple distinct IFN-α genes (13 in man), one to three IFN-β genes (one in man) and other genes, such as IFN-ω, -ϵ, -τ, -δ and -κ. IFN-α and –β genes are induced directly in response to viral infection, whereas IFN-ω, -ϵ, -δ and -κ play less well-defined roles, such as regulators of maternal recognition in pregnancy [21,22]. In this study we use the term type I IFNs to refer to IFN-α/β which are the virally induced cytokines. The rapid production of the type I IFN in response to a viral attack serves as a crucial antiviral defence mechanism in mammals [23-25]. The type I IFN response to invading pathogens is a biphasic phenomenon. First, the detection of viral PAMPs by various PRRs initiates a signalling cascade to activate transcription factors- interferon regulatory factor (IRF)-3 and NF-kB to induce the type I IFNs [26-28]. Second, the IFNs act in an autocrine and paracrine manner to induce interferon stimulated genes (ISGs), the products of which act collectively to interfere with viral replication and spread.

Type II IFN has a single member, also called IFN-γ, and is secreted by activated T cells and natural killer (NK) cells, rather than in direct response to viral infection.

Type III IFN also known as IFN-λ or IL-28 displays IFN-like activities [29,30] by exerting its action through a receptor complex distinct from the type I IFNs [31,32]

IFNs mediate their responses by signalling through distinct but related pathways via specific type 1 or 2 receptors that bind to Janus kinases (JAKs) and subsequently activate signal transducers and activators of transcription (STATs), resulting in expression of a broad range of ISGs. IFN effectors vary widely in their magnitude of inhibitory activity and display combinatorial antiviral properties. Collectively, antiviral ISGs can target almost any step in a virus life cycle. To cite a few examples of those ISGs whose antiviral mechanisms are known, Rsad2 (viperin) prevents influenza A virus egress by perturbing lipid

rafts and promoting TLR7/9 signalling, OAS1/2/3 targets viral replication in flaviviruses by activating RNase L to degrade viral genome, and TRIM25 activate RIG-I signalling to counter viruses such as VSV and influenza A virus. Microarray data and knockout studies have suggested that IFN-induced effectors form a diverse and overlapping landscape. Mice defective in one or more of the classical antiviral pathways (MX1, OAS, and PKR) still mount antiviral responses, indicating that several factors contribute to protection. This redundancy likely reflects the central importance of ISGs in antiviral defence.

2.3 The IRF family functions

Host defences in responses to a viral attack are achieved by the efficient coordination of cellular processes by genetic regulatory networks which ensure rapid alterations in gene-expression programs. The IFN-regulatory factor (IRF) family of transcription factors have been shown to have markedly diverse roles in the gene-regulatory networks of the immune system. The mammalian IRF family comprises nine members: IRF-1, IRF-2, IRF-3, IRF-4, IRF-5, IRF-6, IRF-7, IRF-8 and IRF-9 [33-35]. A brief summary of the roles of each transcription factor in antiviral signalling and responses can referred from **Table 2.**

2.3.1 Roles in signaling

IRFs play important roles in the establishment of signalling pathways that lead to innate immunity. For example- IRF-3 and IRF-7 are early IRFs activated by PRR signalling that play a pivotal role in the initial induction of type I IFNs. Upon activation, IRF-3 and IRF-7 are phosphorylated through the IκB kinase (IKK) family of kinases, dimerised, and translocated into the nucleus to stimulate IFN-β and IFN-α transcription. Following IFN-receptor interaction, a latent cytoplasmic IRF-9 complexes with Stat1 and Stat2 through the activation of the

JAK/STAT pathway, binds to the IFN-stimulated response element (ISRE), and stimulates transcription of a large set of IFN-stimulated genes

Each IRF contains a well-conserved DNA-binding domain of ~120 amino acids which recognises a consensus DNA sequence that is known as the IFN-stimulated response element (ISRE) which can be found on the promoters of ISGs. Thus IRFs also play key roles in the induction of overlapping sets of genes.

2.3.2 Cellular antiviral responses

IRF-1 was the first member to be discovered in the IRF family and the IRF-1 transcription factor was originally identified as a regulator of virus inducible enhancer-like elements of the human IFN-β gene [36]. The consensus IRF-1 binding sequence motif, now termed IRF-E, has been determined to be 5'-G(A)AAAG/CT/CGAAAG/CT/C-3' [37]. Interestingly, sequences related to the consensus IRF-E motif appear within several IFN-stimulated genes (ISG), and for some of these genes, it was shown that IRF-1 directly binds to their promoters and activates transcription. IRF-1 mRNA levels have shown to accumulate in response to IFN, double-stranded RNA (dsRNA), cytokines, and some hormones. IFN-ɣ is the strongest IRF-1 inducer known, although certain combinations, such as IFN-ɣ and tumour necrosis factor-α (TNF-α) induce even higher levels of IRF-1 mRNA[38].

IRF-1 regulates the expression of a number of genes and plays central roles in both innate and adaptive immunity. IRF-1 induces the transcription of many genes involved in the first reaction to viral invasion, such as PKR, OAS, viperin and iNOS [39-42]. IRF-1 also regulates adaptive immune responses by regulation of MHC class I expression and influencing development of NK and T cells [43,44]. Moreover, IRF-$1^{-/-}$ mice have shown influence Th1 responses.

Table 2: A summary of IRF family member functions.

IRFs	Expression	Role in immune and host defences
IRF-1	Constitutive and IFN inducible	• Stimulates expression of ISGs [41,42,45]. • Promotes Th1 responses [46]. • Required for differentiation of CD8+ T cells [47,48]. • Required for NK cell development [44].
IRF-2	Constitutive and IFN inducible	• Antagonizes IRF-1 [49]. • Regulates Th1-Th2 balance [50].
IRF-3	• Constitutive in the cytoplasm • Phosphorylated upon viral infection and then translocated into the nucleus	• Induces Type I IFNs, proinflammatory cytokines and chemokines [51-54]. • Stimulates expression of ISGs [55,56].
IRF-4	• Constitutive in B cells, macrophages. • Inducible by antigen stimulation in T cells and by TLR signalling in macrophages.	• Binds to MyD88 and negatively regulates TLR-dependent induction of proinflammatory cytokine genes [57,58]. • Promotes Th2 differentiation [59,60].
IRF-5	• Constitutive in B cells and DCs. • Inducible by type I IFNs and TLR signalling. • Phosphorylated upon viral infection and then translocated into the nucleus	• Binds to MyD88 and positively regulates TLR-dependent induction of proinflammatory cytokine genes (IL-12p40, IL-6, and TNF-α) [61]. • Induces type I IFNs and proinflammatory cytokines upon virus infection (type I IFNs, IL-6, and TNF-α) [61-63].
IRF-6	Constitutive in skin	Required for keratinocyte differentiation [64,65]
IRF-7	• Constitutive in B cells, pDCs, and monocytes and inducible by type I. • Phosphorylated upon viral infection and then translocated into the nucleus.	• Positively regulates the induction of the type I IFNs [66,67]

IRF-8	• Expressed in macrophages, B cells and DCs and inducible by IFNs	• Required for TLR9 signalling in DCs and macrophages [68]. • Promotes type I IFN production in DCs [69]. • Stimulates IFN-γ- and PAMP-inducible genes [68].
IRF-9	Constitutive and inducible by IFN-γ in various cell types	Binds to STAT1 and STAT2 to form ISGF3 and stimulates type I IFN–inducible genes [70,71]

2.4 Viral evasion strategies

The type I interferon (IFN) system mediates a wide variety of antiviral mechanisms and represents a crucial first barrier to virus infection. However, to generate a productive infection, viruses must overcome antiviral responses, and accordingly, every aspect of these defences is targeted for inhibition. Viruses have thereby developed an impressive diversity of mechanisms to evade the IFN responses.

Several viruses have been found to prevent initial detection by either interfering with the TLR or RLR signalling adaptor proteins such as TRIF or MAVS [72-74]. For example, 3CD protease-polymerase, an intermediate in the polyprotein processing cascade of hepatitis A virus [72] and 3C protein of enterovirus [73] use protease activity to cleave TRIF. The NS3/4A protease of hepatitis C virus, cleaves MAVS off the mitochondria to evade innate immunity [75]. Some viruses can overcome the host responses by manipulating PRR expression levels [76-78] or by even concealing their genetic material to avoid detection [79,80]. In addition, the viruses express proteins that inhibit IFN action on different levels [81-83].

2.5 IRFs driving IFN independent innate immune responses

Host cells have developed strategies to overcome viral evasion mechanisms by adding alternative mechanisms that are not simultaneously declined by the virus. Recent studies have implicated several IFN-independent antiviral mechanisms which bypass viral inhibition of IFN induction and function. Several IRFs have been shown to drive antiviral defence mechanisms independent of the type I IFN signalling *in vitro*. IRF-3 has been shown to induce a subset of ISGs by direct binding to their promoters before IFN itself can be produced [55,84]. In addition, IRF-1 dependent but IFN-independent inductions of antiviral effector functions against different viruses have been shown [42,85]. While mitochondrial MAVS are shown to carry out IFN dependent antiviral mechanisms, peroxisomal MAVS have been shown to induce an immediate albeit transient induction of anti-viral defence factors by IFN independent mechanisms [86]. Further proof of concept included a study which showed IRF-1 mediated induction of several ISGs in $STAT1^{-/-}$ cells [87]. IRF-1 and IRF-5 has also shown to mediate antiviral responses against the hepatitis C virus by an IFN independent mechanism [88]. In addition to the IRF mediated antiviral mechanisms, some ISGs can be directly induced by viral infection in the absence of IFN production [89].

2.6 Immunity in the Central Nervous System (CNS)

The central nervous system (CNS) harbours highly differentiated cells, such as neurons that are essential to coordinate the functions of complex organisms. Numerous cell types act in accord to maintain its integrity and function. The cell types are separated into three main groups: neurons, the glia, and endothelial cells. This organ is partly protected by the blood-brain barrier (BBB) from toxic substances and pathogens carried in the bloodstream. The BBB mechanically separates the CNS from the circulation by the presence of specialised

endothelial cells tightly attached to each other via tight junctions (TJs) and adherens junctions (AJs) [90,91]. The role for these junctions is to restrict and prevent blood-borne molecules and peripheral cells from entering the CNS. Yet, neurotropic viruses can reach the CNS either by infecting epithelial cells on the nasal route leading up to the brain [92], crossing the BBB after viremia [93], by exploiting motile infected cells as Trojan horses [94], or by using axonal transport [95]. For decades, the immune privilege of the CNS was understood as an absence of an immune system inside the CNS, and the BBB was considered only as a barrier isolating the CNS from the peripheral immune system, preventing the entry of infectious agents and immune cells into the CNS [96]. Extensive work in the last decade unravelled the presence of a specialised intrinsic innate immune system in the CNS.

In the case of a viral infection in the brain, pattern recognition receptors (PRRs) recognise pathogen associated molecular patterns (PAMPs) and trigger the onset of antiviral defence mechanisms. The expression of PRRs such as TLRs, RLRs and NLRs have mostly been studied on glia, however, more recent studies have shown neurons to also harbour PRRs [97]. The engagement of such receptors results in the induction of specific pathways and the release of cytokines that play a role in antiviral defences. The engagement of viral PAMPs on TLRs and RLRs are known to drive IFN-β mediated antiviral responses while NLRs are known to drive antiviral responses mediated by IL-1β.

Devoid of a lymphatic system, the integrity of the CNS is guarded exclusively through an innate immune system with an adaptive immunity only present in specific conditions. Classic APCs are normally not found in the CNS [98,99]. Microglia are the resident macrophage like population in the CNS and although they can perform effector inflammatory and APC functions, recent studies report that they originate from the yolk sac unlike hematopoietic cells [100]. Activated T cells are able to infiltrate the CNS, however if the CNS is non-inflamed or if they do not there find a suitable antigen , they leave the CNS again or die by

apoptosis [101]. It is not entirely clear if B- cells can infiltrate to the CNS. Inflammatory responses in the CNS also lead to infiltration of monocytes such as neutrophils, macrophages and dendritic cells.

2.7 Vesicular Stomatitis Virus (VSV)

Many viruses are neurotropic i.e. they are capable of preferentially infecting brain cells. To name a few, west nile virus (WNV), tick borne encephalitis virus (TBEV), measles virus and rabies virus infections can cause severe encephalitic responses in humans that can lead to death. VSV belongs to the family *Rhabdoviridae,* to which the well-known rabies virus also belongs. Transmission of VSV to humans has been documented only once due to laboratory contamination and the experimenter developed flu-like symptoms [102]. It is a common laboratory virus and its replication mechanism is well understood in several cell culture systems. Therefore, it has for decades been used as a model for neurotropic virus infections in mice [103]. VSV is an enveloped single stranded negatively sensed rod shaped RNA virus coding for 5 proteins i.e. glycoprotein (G), large protein (L), phosphoprotein (P), matrix protein (M) and nucleoprotein N. Its genome is associated with N, L and P proteins to form the nucleocapsid. Together the L and P proteins form the RNA dependent RNA polymerase that is involved in the transcription of the genome [104]. The M protein is involved in the later steps of viral replication and condenses the nucleocapsid to a tightly coiled structure. The outer membrane of virion is the envelope composed of a cellular lipid bilayer. The transmembrane G protein is anchored in the viral envelope, which is essential for receptor binding and cell entry [105]

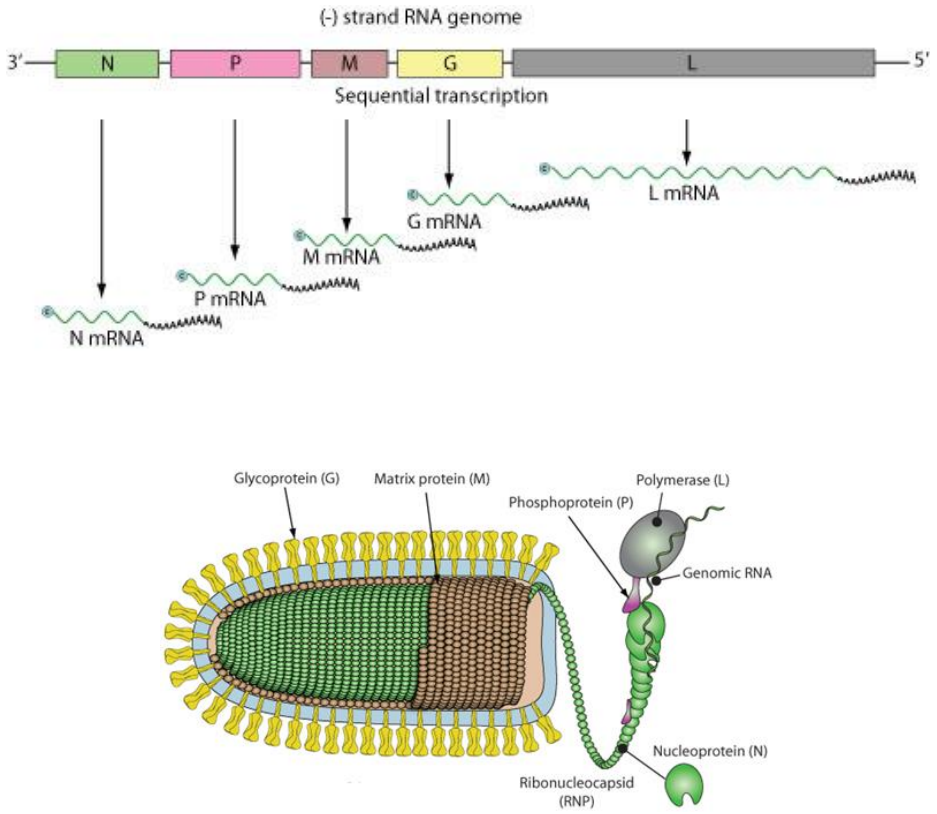

Figure 1: Genome organisation and packaging of VSV (adapted from http://viralzone.expasy.org/)

Negative-stranded RNA linear genome; about 11 kb in size. Encodes for 5 proteins. Enveloped, bullet shaped, 180 nm long and 75 nm wide.

Like nearly all viruses, VSV can also evade type I IFN action [106,107]. The M protein plays a major role in the virus-induced inhibition of host gene expression. It has been proposed that the inhibition of host gene expression by M protein is responsible for suppressing activation of host IFN gene expression. Most wild-type strains of VSV induce little if any interferon gene expression, while mutant viruses such as AV2 which have a mutation in the M protein can mount a normal IFN response [106,107]. WT VSV M protein suppresses interferon gene expression by inhibiting host RNA and protein synthesis.

3 AIM OF THIS WORK

VSV is a cytopathic virus, belonging to the family *Rhabdoviridae*, capable of causing encephalitis in mice. Type I IFN is rapidly induced upon infection and is crucial to prevent death [108]. In fibroblast cells, type I IFN production and action is efficiently blocked by the virus [109]. Previous results demonstrate that IRF-1 mediated an antiviral response in the absence of type I IFN induction by direct transcriptional activation of ISGs [42,86].

In this study we aimed to uncover the role of IRF-1 mediated antiviral responses by IFN independent mechanisms *in vivo*. Since VSV is a neurotropic virus, we questioned if IRF-1 had a particular role of executing antiviral innate responses in the CNS. Our efforts were aimed to uncover the mechanisms by which neurotropic viral infections are cleared by IRF-1 dependent mechanisms. We also aimed to uncover the cell types in the brain which execute these responses. Moreover the extents to which the IRF-1 mediated antiviral responses are essential to the host were also investigated.

4 RESULTS

In the past years, many studies have demonstrated the role of the IRFs in coordinating innate immune signalling events downstream of PRR signalling and regulating the IFN response. However, certain factors such as IRF-1 have been shown to mediate antiviral responses by inducing ISGs by IFN independent mechanisms as well. VSV is a neurotropic virus of the *Rhabdoviridae* family that efficiently blocks type I IFN induction and function *in vitro*. Thus by using the model of VSV infections in vivo, we aim to uncover the separate roles of IRF and IFN in antiviral defences.

4.1 IRFs play a crucial role to defend against VSV infections

To investigate the role of various IRFs in mediating antiviral responses i*n vivo*, we used gene knockout mice to study their increased susceptibility to VSV. WT mice infected intranasally (i.n.) with 10^7 plaque forming units (pfu) of VSV displayed a mere 20% mortality **(Figure 2)**. In contrast, IRF-$3^{-/-}$ and IRF-$7^{-/-}$ mice were found to be susceptible to i.n. VSV infections with sublethal doses of 10^6 pfu, displaying 100% mortality. IRF-$5^{-/-}$ mice are also previously shown to be susceptible to VSV infections [62]. IRF-$1^{-/-}$ mice were also found to be susceptible to VSV infections, displaying 100% mortality and were dead within 7 days after showing sign of encephalitis. These data show that many of the IRF family members play a crucial role in antiviral defences against VSV. To also study the importance of the type I IFN response in antiviral defences, type I IFN receptor knockout i.e. $IFNAR^{-/-}$ mice were also used in the study. As these mice

are previously reported to be very susceptible to many virus infections, they were infected i.n. with a low dose of 10^2 pfu of VSV. Despite the administration of low VSV doses, all IFNAR$^{-/-}$ mice died very early i.e. within 3 days. These data confirm that type I IFN plays a crucial role in the early and immediate responses against VSV infection. Importantly, we conclude that IRFs are also pivotal for survival of VSV infection, albeit at higher infectious doses and at slightly later time points of the infection.

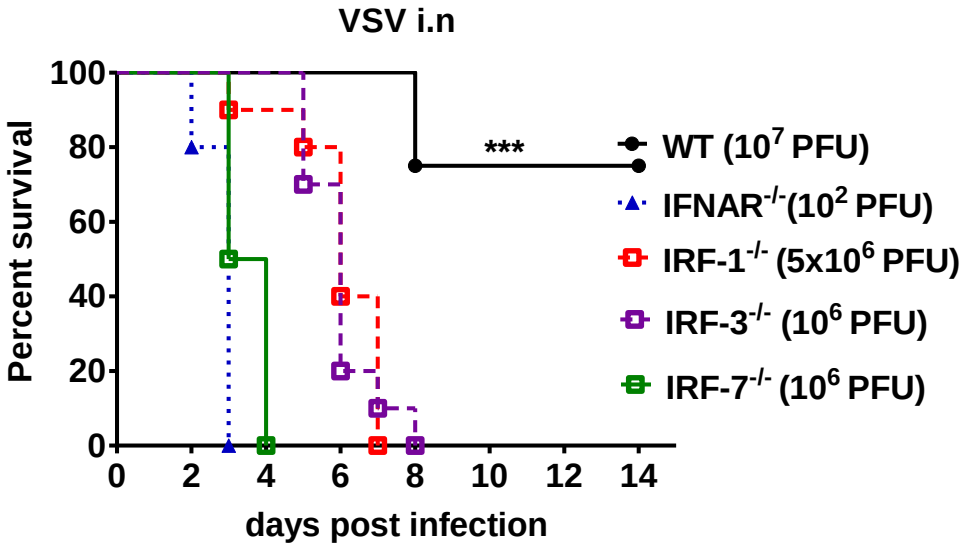

Figure 2: IRFs protects mice from lethal intranasal VSV infection

Survival analysis of WT (n=12), IFNAR$^{-/-}$ (n=5), IRF-1$^{-/-}$ (n=10), IRF-3$^{-/-}$ (n=10) and IRF-7$^{-/-}$ (n=10) mice, infected i.n. with VSV at doses as indicated in the figure. Data are representative of at least two independent experiments. Survival differences were tested for statistical significance by the log-rank test.

4.2 IRF-1 has a special antiviral action in the brain upon VSV infection

We previously demonstrated that IRF-1 mediates a type I IFN independent antiviral response against VSV *in vitro* [42], which proves to be essential when viruses evade innate immune responses by antagonizing the induction and

function of the type I IFN system. Upon intranasal infection VSV enters the CNS by directly infecting the olfactory receptor neurons [92]. Since VSV is a neurotropic virus, we wanted to analyse if the IRF-1 mediated antiviral action was necessary to combat neuropathogenesis *in vivo.* Therefore to investigate if IRF-1 plays a specific role in neurotropic VSV infection we compared systemic and CNS infection by infecting them via different routes i.e. i.n. for a neurotropic infection and i.v. for a systemic infection. IRF-$1^{-/-}$ mice were found to be susceptible to i.n. VSV infection at sub lethal doses **(Figure 2)**. In contrast, systemic VSV infection of IRF-$1^{-/-}$ mice showed no increased susceptibility in comparison to WT mice **(Figure 3A)**. IFNAR$^{-/-}$ mice were very susceptible to systemic VSV infections and died within 3 days. Interestingly, intranasal infection of mice infected with the non-neurotropic Influenza PR-38 virus had little impact on the survival of IRF-$1^{-/-}$ mice, as most of them survived the infection, similar to the infected WT mice **(Figure 3B)**. These data indicate that while type I IFN responses are essential to protect from both neurotropic and systemic VSV infections, IRF-1 mediated antiviral responses are crucial only for neurotropic VSV infections.

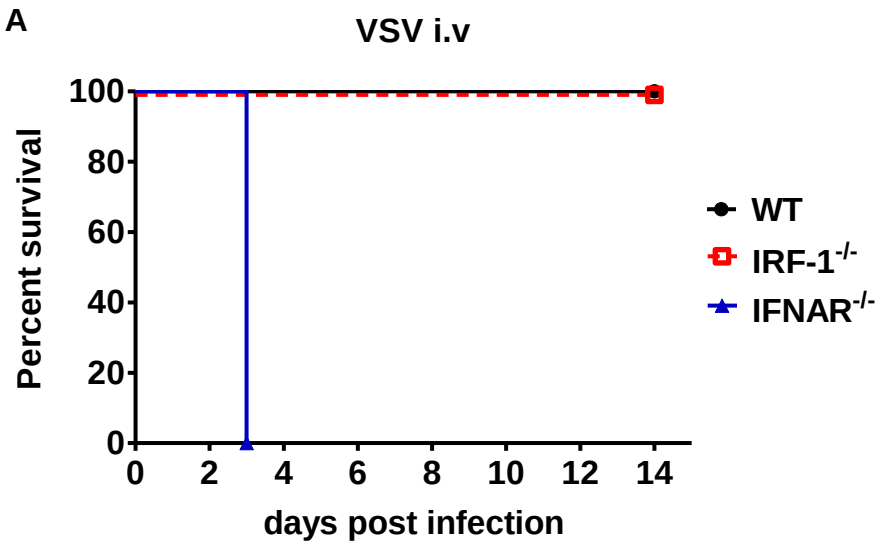

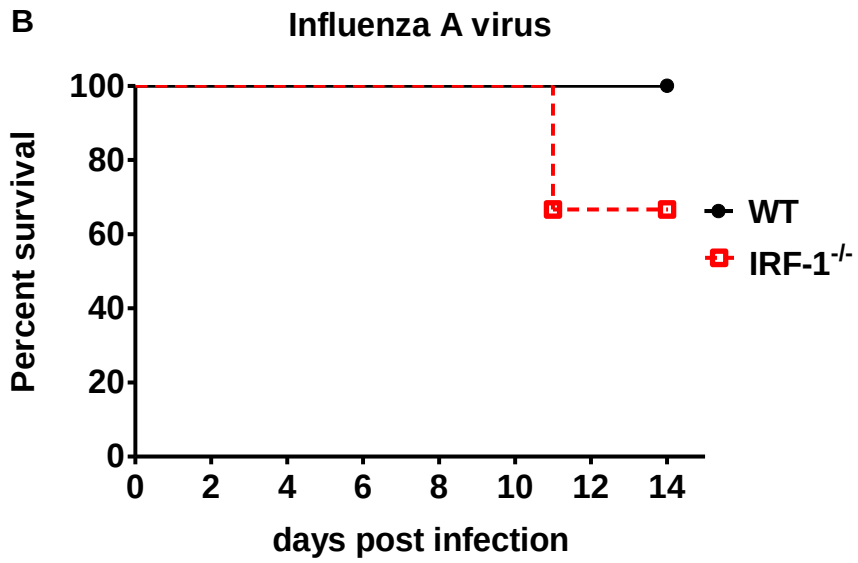

Figure 3: IRF-1 has a specific antiviral action in the brain.

A, Survival curves of WT (n=5) , IRF-$1^{-/-}$ (n=6) and IFNAR$^{-/-}$ (n=5) mice after i.v. infection with 5 x 10^6 pfu VSV. B, Survival curves of WT and IRF-$1^{-/-}$ mice after intranasal infection with 0.04 MLD50 Influenza A virus PR8/A/34.
Data are representative of at least two independent experiments. Survival differences were tested for statistical significance by the log-rank test.

4.3 IRF-1 is not a regulator of type I IFN or type III IFN

VSV replication is reported to be controlled by type I IFN [108,110]. Previous studies with other viruses have implied IRF-1 as an activator of IFN-α/β gene transcription in cell culture [111].Therefore, we determined the impact of IRF-1 on the IFN response upon VSV infection. To this end, we determined IFN-α serum levels in VSV infected mice **(Figure 4)**. Equal levels of IFN-α were detectable in the serum of both WT and IRF-$1^{-/-}$ mice at 6 hours and 24 hours post infection. However, IRF-$1^{-/-}$ mice displayed higher IFN-α in the serum 2 days post infection. No IFN-α was detectable in WT and IRF-$1^{-/-}$ mice from day 4 post infection.

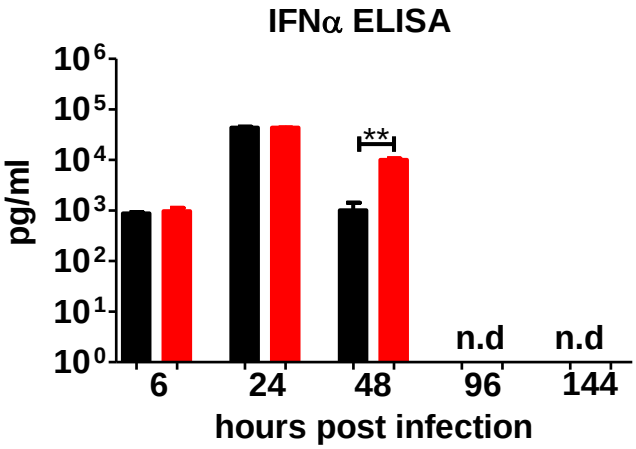

Figure 4: IRF-1 is not a regulator of IFN-α.

Mice were infected i.n. with 5 x 10^6 pfu of VSV. Serum was collected from WT and IRF-$1^{-/-}$ mice 6, 24, 48, 96 and 144 hours post infection. IFN-α protein was detected by ELISA. Data represents mean with SEM of 5-6 mice in each group per time point. Asterisks indicate statistical significance calculated by Mann-Whitney test, ** $p<0.005$.

To determine the impact of IRF-1 in IFN-β production, we took advantage of an IFN-$\beta^{+/\Delta\beta\text{-luc}}$ reporter mouse [112], which allows tracking of IFN-β gene induction *in vivo*. Intranasal VSV infection of IFN-$\beta^{+/\Delta\beta\text{-luc}}$, IRF-$1^{+/-}$IFN-$\beta^{+/\Delta\beta\text{-luc}}$, IRF-$1^{-/-}$IFN-$\beta^{+/\Delta\beta\text{-luc}}$ showed no differences of reporter gene expression within them **(Figure 5).** The signal reached its maximum, 48 hours post infection after which it declined. Since the IFN- β levels are not differentially regulated between WT and IRF-$1^{-/-}$mice we conclude that IRF-1 is not a regulator of IFN-β.

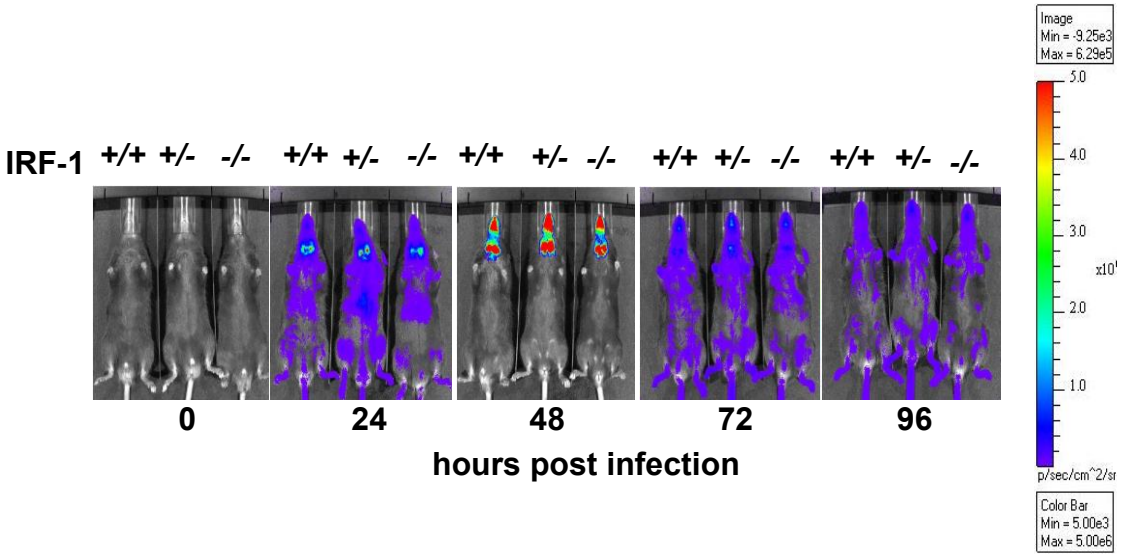

Figure 5: IRF-1$^{-/-}$ mice have no defects in induction of IFN- β

IFN-β$^{+/\Delta\beta\text{-luc}}$, IRF-1$^{+/-}$ IFN-β$^{+/\Delta\beta\text{-luc}}$, IRF-1$^{-/-}$ IFN-β$^{+/\Delta\beta\text{-luc}}$ transgenic mice were i.n. infected with 5x10^6 pfu of VSV and subjected to whole body imaging. Mice were imaged before treatment (0h) and over time as indicated. Images from a representative mouse are shown. The rainbow scale indicates the number of photons measured per second per cm^2 per steradian (sr).

We could previously demonstrate that IRF-1$^{-/-}$ mice had no deficiency in their type I IFN activity in comparison to WT mice **(Figure 4/5)**. To further investigate with IRF-1 had any impact on the induction of type III IFNe also took advantage of a MX2Luc reporter mouse which allows whole body *in vivo* imaging of type I and III response using firefly luciferase as a reporter [113]. Both type I and type III IFNs can specifically induce the MX2 gene and since the MX genes in inbred mouse strains are not functionally translated and, the disruption or manipulation of these genes should not significantly alter cellular functions [114,115]. Since, the type I IFN levels are not altered between WT and IRF-1$^{-/-}$ mice, any difference in luciferase expression detected would be contributed by the type III IFN. Intranasal VSV infection of IRF-1$^{+/-}$MX2luc induced reporter gene expression in the whole body, with a major response in the region of the liver 24

hours post infection **(Figure 6A).** The signal reached its maximum, 48 hours post infection after which it declined. No differences of luciferase signals was detectable in IRF-$1^{+/+}$Mx2Luc mice (data not shown), IRF-$1^{+/-}$MX2luc and IRF-$1^{-/-}$ MX2luc mice. Detailed analysis of luciferase expression in different organs revealed a slightly higher type I IFN response in some organs of IRF-$1^{-/-}$ mice compared to WT controls **(Figure 6B)**. In WT mice the IFN responses in the brains were back to basal levels by day 9 post infection. These results confirmed that a lesion in the IRF-1 gene does not lead to diminished levels of Type I IFN. This corroborates the evidence that there is no deficiency in IFN action and is not responsible for the increased susceptibility of IRF-$1^{-/-}$ mice.

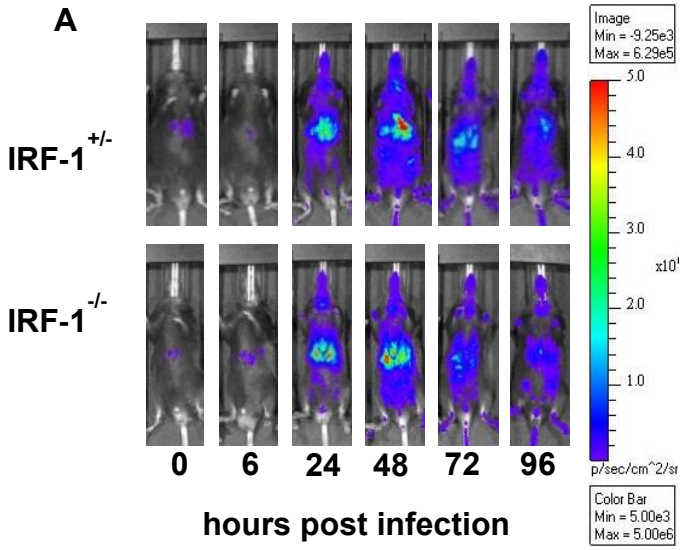

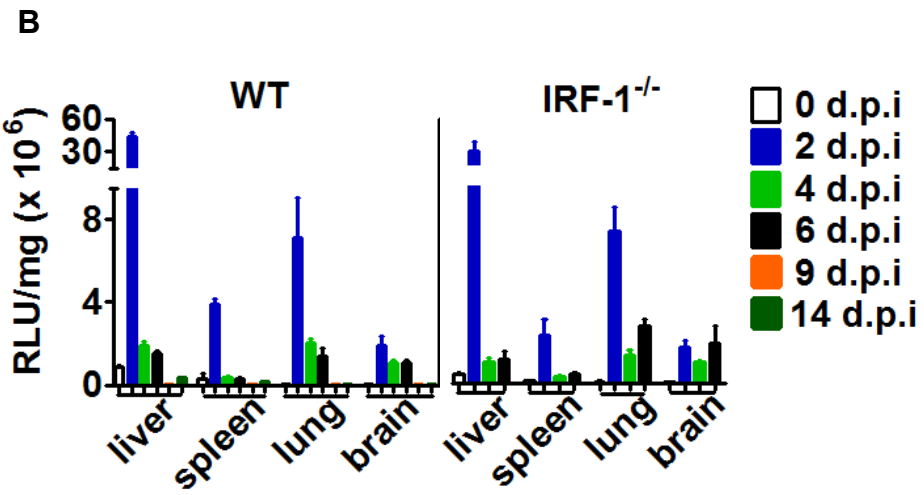

Figure 6: Systemic type I IFN response cannot rescue IRF-1$^{-/-}$ mice from VSV infections.

IRF-1$^{+/-}$MX2luc and IRF-1$^{-/-}$MX2luc transgenic mice were infected i.n. with 5x10^6 pfu of VSV. A. Mice were subjected to whole body imaging. Mice were imaged before treatment (0h) and over time as indicated. Images from a representative mouse are shown. The rainbow scale indicates the number of photons measured per second per cm^2 per steradian (sr).B, Luciferase activity from the homogenized organs of uninfected or infected IRF-1$^{+/-}$MX2luc and IRF-1$^{-/-}$MX2luc transgenic mice were quantitated at indicated days post infection (d.p.i).
Data represents mean with SEM of 4-8 mice in each group per time point.

4.4 Both IRF-1 and type I IFN responses are crucial for antiviral responses against VSV in the CNS

Since VSV is a neurotropic virus, we investigated the impact of IFN and IRF-1 dependent antiviral responses in the CNS. To this end we made use of conditional IFNAR$^{fl/fl}$NesCre$^{+/-}$ mice that suffer from the IFNAR deletion specifically in neuroectodermal cells of the CNS such as neurons and astrocytes

but not microglia [116]. A previous study reported that i.n VSV infection of IFNAR$^{fl/fl}$NesCre$^{+/-}$ led to their death in 6 days [108]. Infection of these mice with a dose of 5x10^{6} pfu of VSV, IFNAR$^{fl/fl}$NesCre$^{+/-}$ succumbed to the infection by 6 days post infection after dramatic experiencing weight loss **(Figure 7)**. With this we conclude that type I IFNs are a potent antiviral defence mechanism against neurotropic VSV infections.

To investigate if IRF-1 can also execute antiviral actions in the CNS independent of the type I IFN signalling, IRF-1$^{-/-}$IFNAR$^{fl/fl}$NesCre$^{+/-}$ were infected with the same dose of VSV and their survival kinetics were followed. IRF-1 deficient IRF-1$^{-/-}$IFNAR$^{fl/fl}$NesCre$^{+/-}$ mice succumbed to the infection within day 2 and 5 post infection which was earlier than the fate of IFNAR$^{fl/fl}$NesCre$^{+/-}$ mice **(Figure 7)**. This indicates that apart from the IFN system, IRF-1 is able to execute additional antiviral functions in the brain. Together, these data suggest a pivotal antiviral function of both IRF-1 and type I IFN in the brain. The data also suggest both IFN and IRF-1 can execute their activities independent of one another.

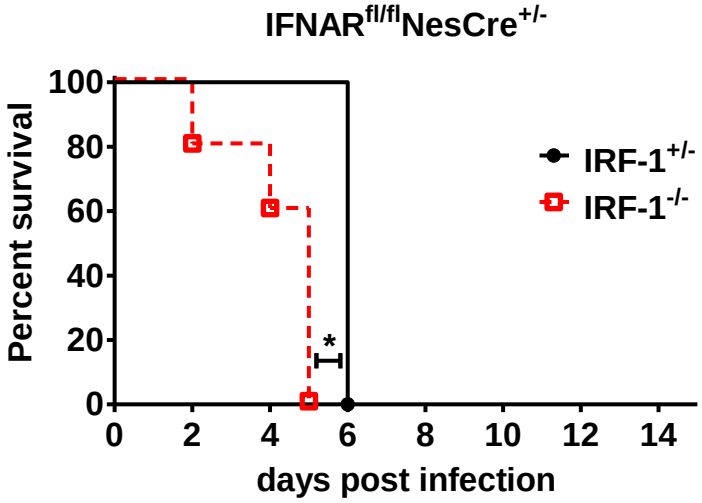

Figure 7: The action of IRF-1 is independent of the type I IFN

Mice were infected intranasally with 5 x 10^6 pfu of VSV. Survival analysis of IRF-1 sufficient (IRF-$1^{-/-}$) (n=3) or deficient (IRF-$1^{-/-}$) (n=5) IFNAR$^{fl/fl}$NesCre$^{+/-}$ mice.
Statistical significance was calculated by the log-rank test.

4.5 IRF-1 mediated antiviral response is independent of the B cell responses.

Earlier work has demonstrated the importance of adaptive immune system for survival during VSV infection. In particular, a depressed neutralizing antibody response in the periphery promotes early dissemination of the virus to the CNS [37]. To assess if the severe phenotype of IRF-$1^{-/-}$ mice post VSV infection was due to an ill antibody response, we evaluated whether IRF-1 modulates the humoral immune response by determining VSV neutralizing antibodies **(Figure 8)**. Similar levels of VSV specific IgM and IgG titres were detected in IRF-$1^{-/-}$ and WT mice. These data suggest that the increased viremia in the CNS of the IRF-$1^{-/-}$ is not due to a defect in the B cell response.

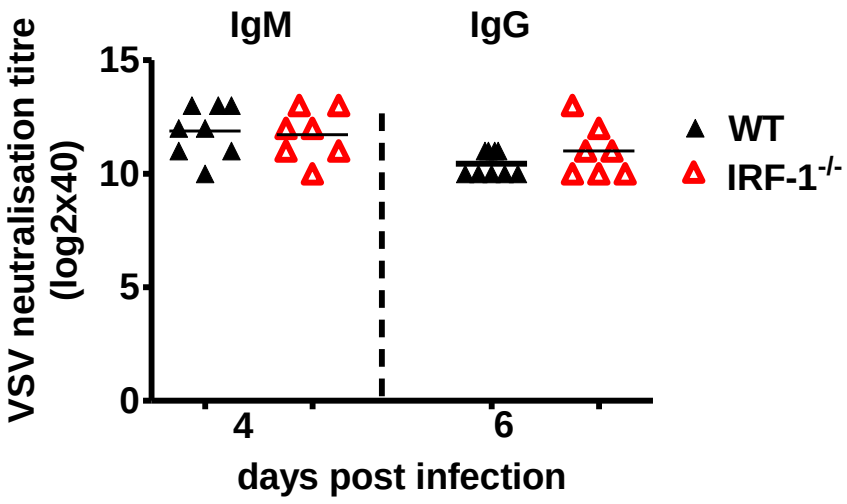

Figure 8: The antiviral effects of IRF-1 are not driven by the B cell response

WT and IRF-$1^{-/-}$ mice were infected intranasally with 5 x 10^6 pfu VSV and serum samples were collected at the indicated time points. Virus specific IgM and IgG titres were quantitated by the virus neutralization assay.

4.6 IRF-1 mediated antiviral responses are independent of T cell mediated responses

Previous studies have demonstrated that T cells are required for the long term survival of VSV infection. IRF-1 transcriptionally regulates the expression of certain MHC class I molecules such as LMP-2, TAP-1. As a result MHC class I cell surface expression is decreased in IRF-$1^{-/-}$ mice [43,47]. Moreover, IRF-$1^{-/-}$ mice fail to mount a normal Th1 response upon a pathogen challenge because IRF-1 transcriptionally regulates the p40 subunit of IL-12 [46,117]. As a result, naïve IRF-$1^{-/-}$ mice display defects in the frequency of CD8+ T cells in peripheral organs such as the spleen **(Figure 9A)**. The defects are also consistent when the total CD8+ T cells are quantitated in cell numbers from the spleen **(Figure 9B)**. Although the frequency of CD4+ T cells in the spleen seem higher in the

IRF-1$^{-/-}$ mice, no differences in CD4 cell numbers were found between the WT and IRF-1$^{-/-}$ mice (data not shown).

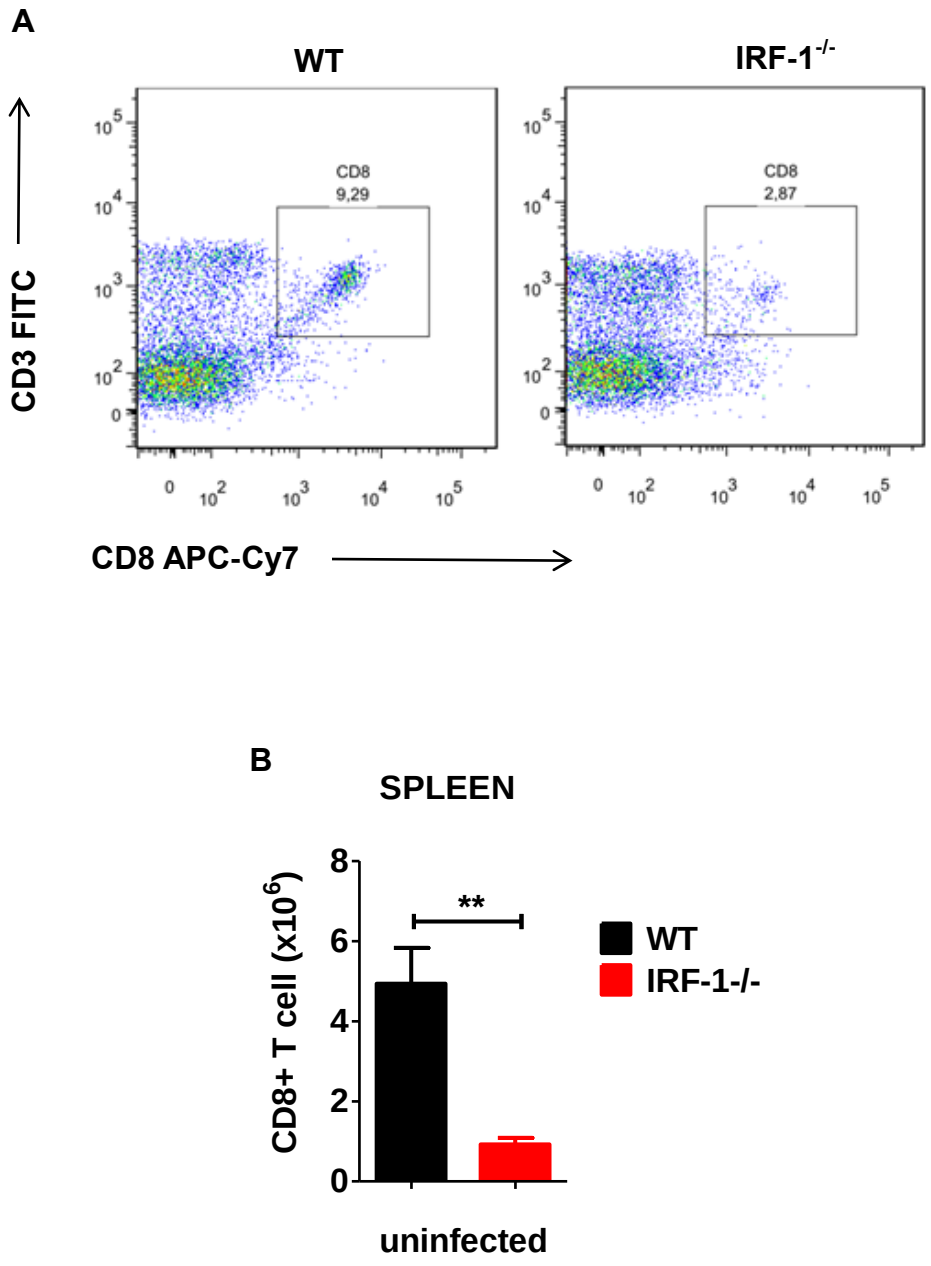

Figure 9: IRF-1$^{-/-}$ mice have lower numbers of CD8+ T cells

A, Representative flow cytometry profiles of spleen CD3^{+}CD8^{+} T cell staining from uninfected WT and IRF-1$^{-/-}$ mice are shown. B, Total numbers of CD8^{+}T cells in the spleen of WT and IRF-1$^{-/-}$ are shown.
Asterisks indicate statistical significance calculated by Mann-Whitney test, ** p<0.005.

Since i.n. infection of VSV leads to viral replication in the brain [108], infiltration of T cells in the brain as a part of the host immune response were expected. We compared the levels of $CD8^+$ T cells infiltrating the brains of IRF-$1^{-/-}$ and WT mice. Significantly lesser frequencies as well as numbers of $CD8^+$ T cells infiltrated the brain of IRF-$1^{-/-}$ mice **(Figure 10A/B)**. The lesser numbers of infiltrating $CD8^+$ T cells is likely due to the lesser numbers of $CD8^+$ T cells in these mice.

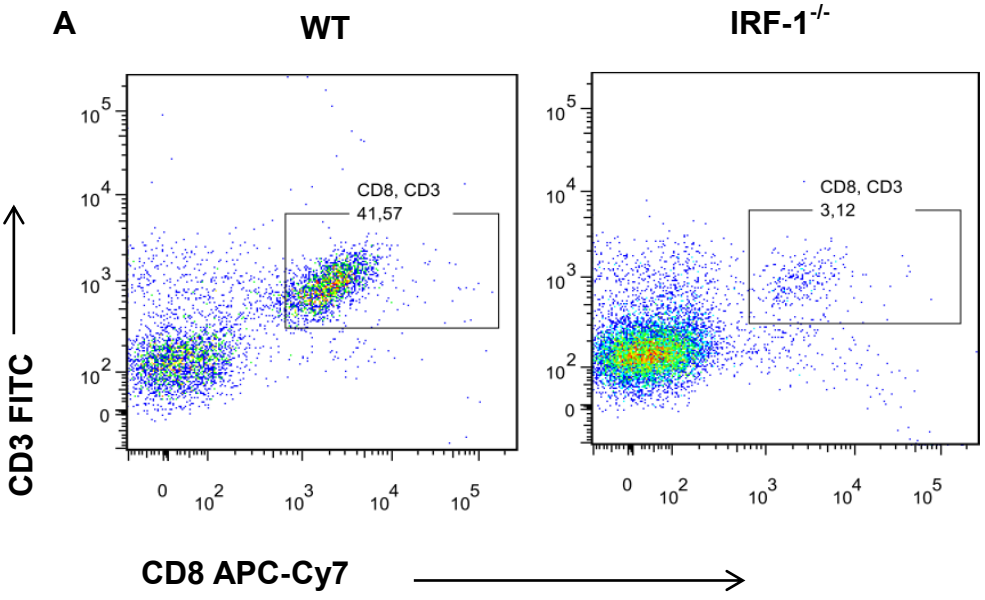

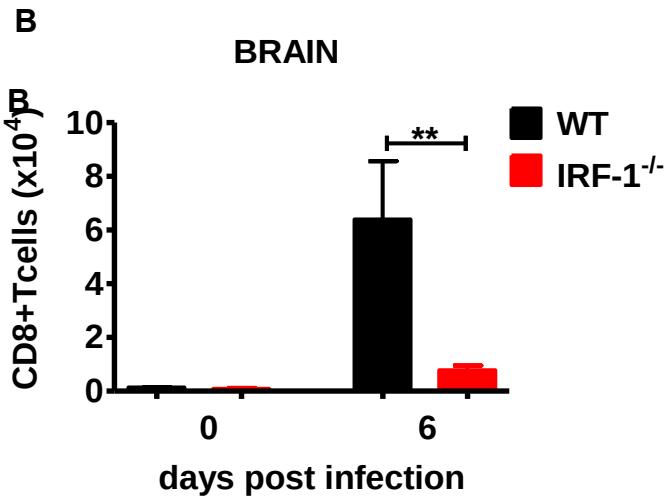

Figure 10: Infected IRF-1$^{-/-}$ mice have lesser numbers of CD8^{+} T cells infiltrating the brain

Mice were infected i.n with 5x10^{6} pfu of VSV.A, Representative flow cytometry profiles of brain infiltrating CD3+CD8^{+} T cells from 6 days post infected WT and IRF-1$^{-/-}$ mice are shown.B, Total numbers for CD8^{+} T cells in the brains of uninfected and 6 days post infected WT and IRF-1$^{-/-}$ mice were evaluated.
Asterisks indicate statistical significance calculated by Mann-Whitney test, ** p<0.005.

T cells are known to play a role in the long term survival after VSV infection. To investigate the impact of the lower T cell number in IRF-1$^{-/-}$ mice we adoptively transferred WT T cells into IRF-1$^{-/-}$ mice. T cells were isolated from the spleens of WT mice expressing a congenic marker Thy1.1 and then transferred into both WT and IRF-1$^{-/-}$ mice. 2 days post transfer the number of WT Thy 1.1 cells were analysed in the IRF-1$^{-/-}$ mice **(Figure 11 A)** and then subsequently infected. IRF-1$^{-/-}$ mice that were supplemented with T cells did not show any improvement in their survival rate post i.n. VSV infection and still died in 6 days **(Figure 11B)**.

Therefore we conclude that in this model of VSV infection, T cell response have no impact in IRF-1 mediated antiviral response.

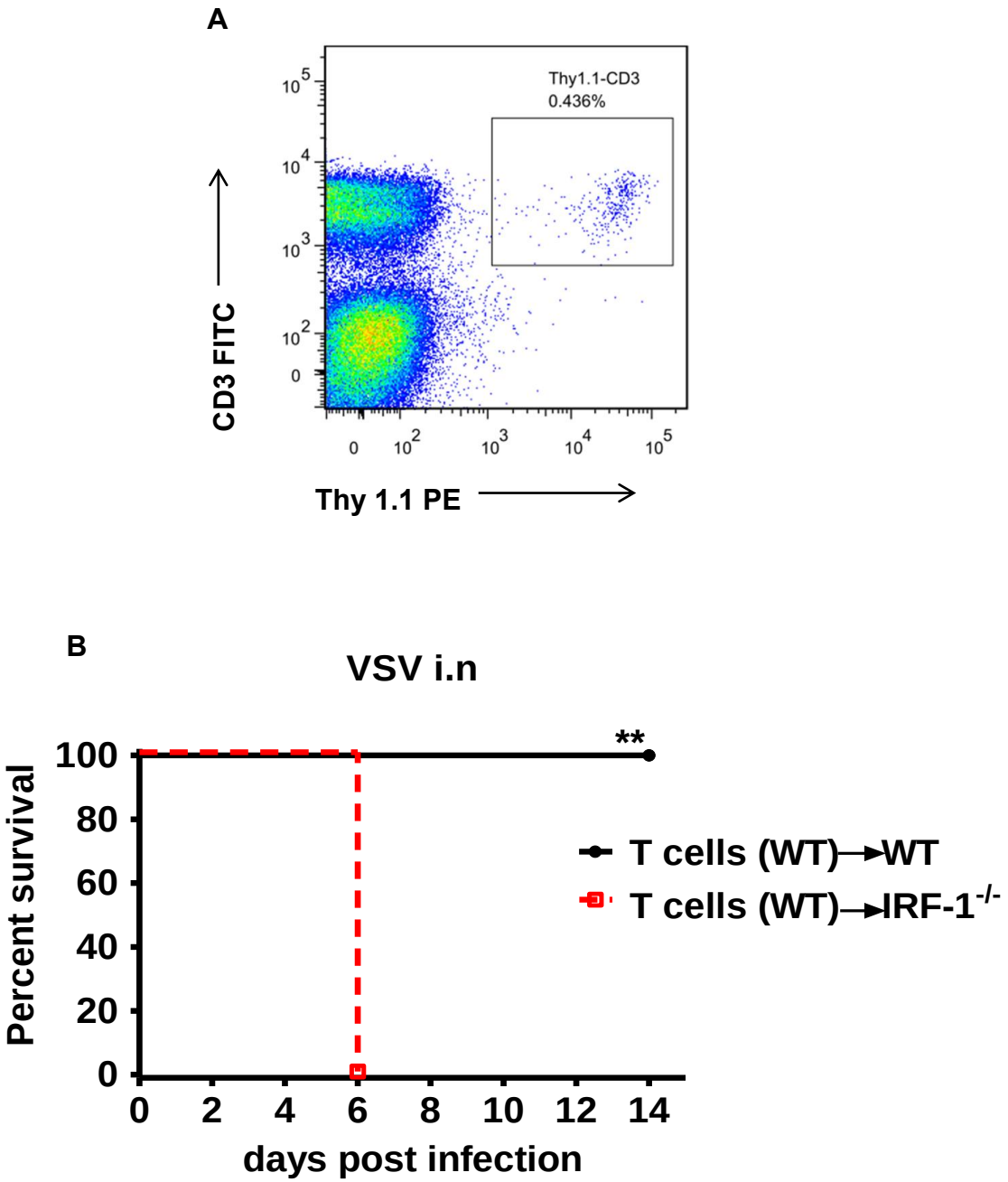

Figure 11: The anti-viral effects of IRF-1 are not driven by CD8$^+$ T cells.

A, Representative flow cytometry profiles of Thy 1.1-CD3$^+$ WT T cells in spleens of IRF-1$^{-/-}$ mice 2 days post transfer. B, Survival analysis of WT (n=5) and IRF-1$^{-/-}$ (n=4) mice adoptively transferred with 10^7 T (Thy1.1) cells, 2 days prior to intranasal infection with $5x10^6$ pfu VSV. Survival differences were tested for statistical significance by the log-rank test.

4.7 IRF-1 mediated antiviral responses are mediated by the brain resident cells

While the systemic IFN response and neutralizing antibodies have no impact on the IRF-1 mediated antiviral responses, we asked if the antiviral action of IRF-1 is due to stromal and brain resident cells or the hematopoietic system facilitates an indirect control of VSV infection. Since the hematopoietic cells are sensitive to irradiation while the brain resident cells are resistant [40], we established reciprocal bone marrow chimeric mice by lethal irradiation of CD45.1 WT or CD45.2 IRF-$1^{-/-}$ mice, followed by adoptive transfer. After 6-8 weeks, we tested the mice for chimerisms and found that the donor cells had replenished the bone marrow **(Table 6)** and then subsequently infected i.n. with VSV. WT → WT chimeras were a little bit more susceptible than WT mice but 70% were capable of limiting infection. IRF-$1^{-/-}$ → WT showed comparable susceptibility to VSV infection like WT → WT mice, while WT → IRF-$1^{-/-}$ chimeras were unable to rescue the IRF-$1^{-/-}$ mice **(Figure 12A)**. This suggests that loss of IRF-1 expression in haematopoietic cells has no impact on survival of the mice while IRF-1 expression in host stromal and resident brain cells is critical to control the virus.

To investigate if WT → IRF-$1^{-/-}$ chimeras are more susceptible due to differences in the recruitment of lymphocytes compared to the WT → WT chimeras, we analysed brain infiltrating T cells in the chimeric mice. The data revealed no differences in the number of donor $CD8^+$ T cells between WT → WT and WT → IRF-$1^{-/-}$ chimeras **(Figure 12 B/C)**. Moreover, $CD8^+$ T cells in the brains of IRF-$1^{-/-}$ or WT recipients were neither activated nor antigen specific (data not shown). Thus, the IRF-1 mediated antiviral effects are driven primarily by radiation-resistant stromal or brain resident cells.

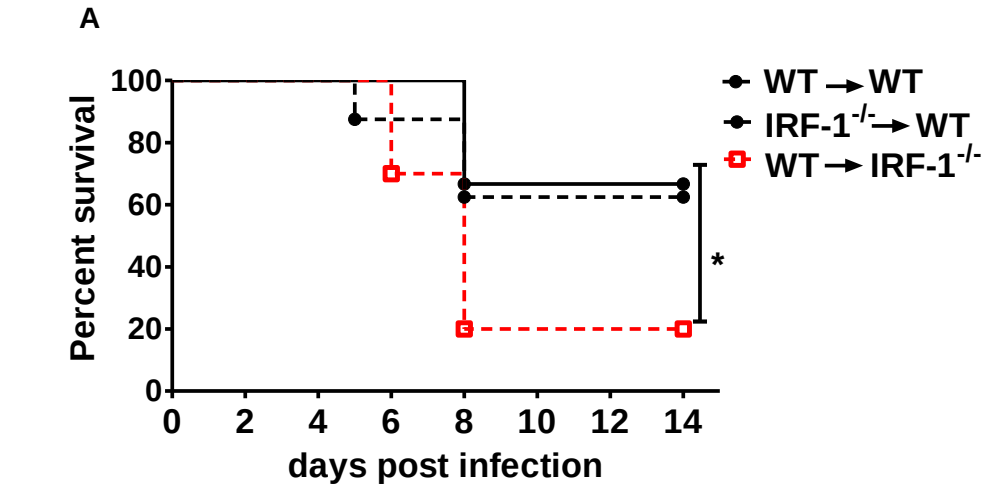
A
Percent survival
100
80
60
40
20
0
0
2
4
6
8
10
12
14
days post infection
WT → WT
IRF-1-/- → WT
WT → IRF-1-/-
*

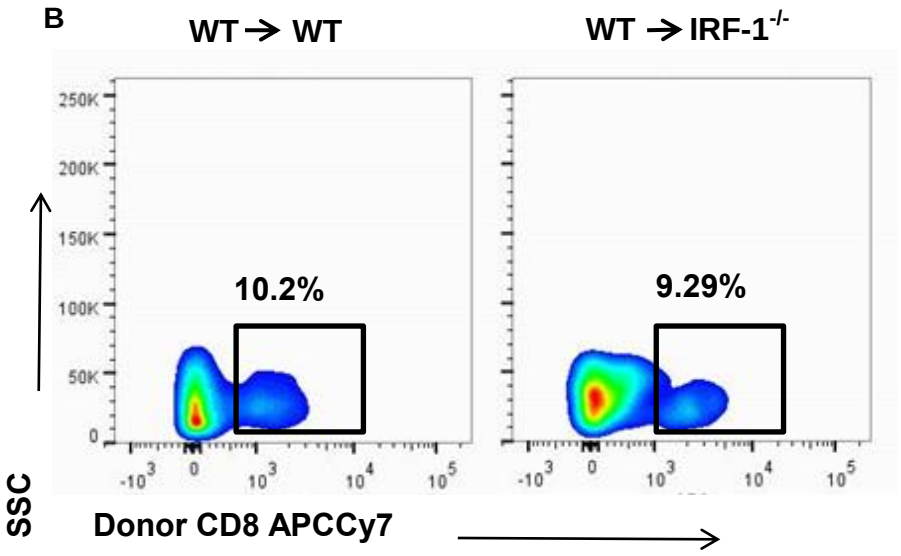
B
WT → WT
WT → IRF-1-/-
250K
200K
150K
100K
50K
0
10.2%
9.29%
SSC
Donor CD8 APCCy7

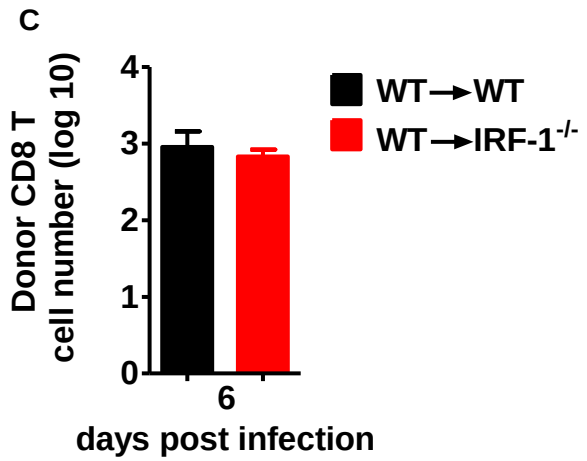

Figure 12: The anti-viral effects of IRF-1 are neither driven by the adaptive immune responses nor by the hematopoietic cells.

WT and IRF-1$^{-/-}$ mice were lethally irradiated and reconstituted with bone marrow from IRF-1$^{-/-}$ or WT mice. Mice were tested for their chimerism after 6-8 weeks and i.n. infected with 5 x 10^6 pfu. A, Survival was monitored and plotted as Kaplan-Meier curves (n=8-10). Data are representative of two independent experiments. Survival differences were tested for statistical significance by the log-rank test, * $p<0.05$. B, C Leukocytes were isolated from brains of chimeric mice (n=6-9) 6 days post infection, stained for CD45.1 and CD8, and analysed by flow cytometry, B, Representative flow cytometry profiles of WT CD8$^+$ T cells from donor hematopoietic cells in the recipient irradiated WT and IRF-1$^{-/-}$ mice. C, Total cell numbers for infiltrating donor WT CD8+ T cells in the brains of WT and IRF-1$^{-/-}$ mice.

4.8 The antiviral effects of IRF-1 are dispensable for clearance in the peripheral organs

Intranasal administration of a high viral dose of VSV leads to viral replication in the brain as well as in peripheral organs where it first reaches the lung and then disseminates to the other tissues [108]. We therefore determined viral load from various peripheral tissues by plaque assay 2, 4, 6 days post intranasal infection with 5 x 10^6 pfu of VSV **(Figure 13)**. VSV titres were quantitated as plaque forming units per gram (pfu/g) from the peripheral organs. Viral titres were higher in the. liver, spleen and lungs of IRF-1$^{-/-}$ mice in comparison to WT mice

(248.8, 466.5 and 5,64 fold higher respectively), 2 days post infection. However, viral clearance from the liver and spleen of both WT and IRF-$1^{-/-}$ mice was observed by day 4. Higher VSV titres were found in the lung than the other tissues but were cleared by day 6 post infection. These data indicate that IRF-1 had an impact in limiting viral replication but clearance of the virus from peripheral organs could be achieved even in the absence of IRF-1.

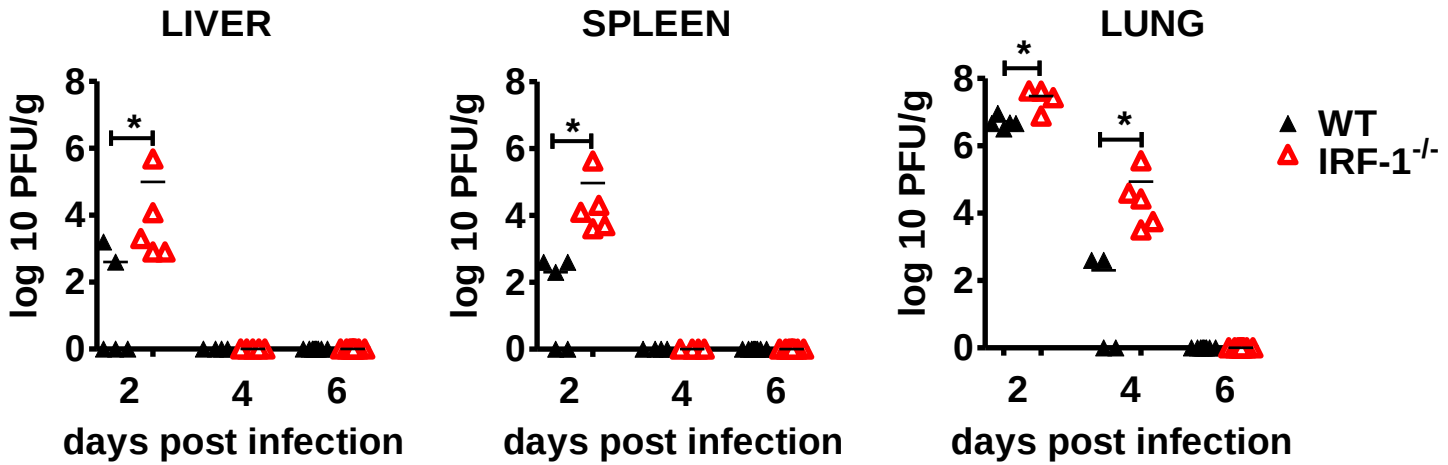

Figure 13: IRF-1 mediated antiviral effects are dispensable in the peripheral organs.

WT and IRF-$1^{-/-}$ mice were infected i.n. with 5 x 10^6 pfu of VSV. Viral burden was quantitated by plaque assay from peripheral organs- liver, spleen and lung. Data are representative of at least two independent experiments.
Asterisks indicate statistical significance calculated by Mann-Whitney test, * $p<0.05$.

4.9 Dynamics of viral replication in the brain of w.t. and IRF-1$^{-/-}$ mice

Intranasal administration of VSV leads to spread from the nasal cavity to the olfactory bulb and into the CNS [92,118]. To examine the impact of IRF-1 in brain infection in more detail, we determined the viral load in different brain parts, i.e olfactory bulb, cerebrum, cerebellum and brain stem **(Figure 14)**. At 2 days post infection, viral titres of WT mice were highest in the olfactory bulb ($2.087x10^6$pfu/g) compared to the cerebrum ($1.22x10^5$ pfu/g), cerebellum ($1.34x10^5$ pfu/g) and the brain stem ($1.15x10^5$ pfu/g), 2 days post infection. WT mice cleared the virus within 6 days. At 2 days post infection IRF-1$^{-/-}$ mice had similar titres to WT mice which declined by 4. However by day 6, only the olfactory bulb could clear the virus with similar kinetics compared to the peripheral tissues and a surge of viral load was found in the brain tissues of IRF-1$^{-/-}$ mice. High viral titres developed at this time point in the cerebrum, cerebellum and brain stem, suggesting this as a cause for the death of these animals. These data indicate that IRF-1 plays a negligible role during the early phase of viral brain infection and clearance. However, IRF-1 is crucial in the control of a second phase of viral replication in the cerebrum, cerebellum and brain-stem.

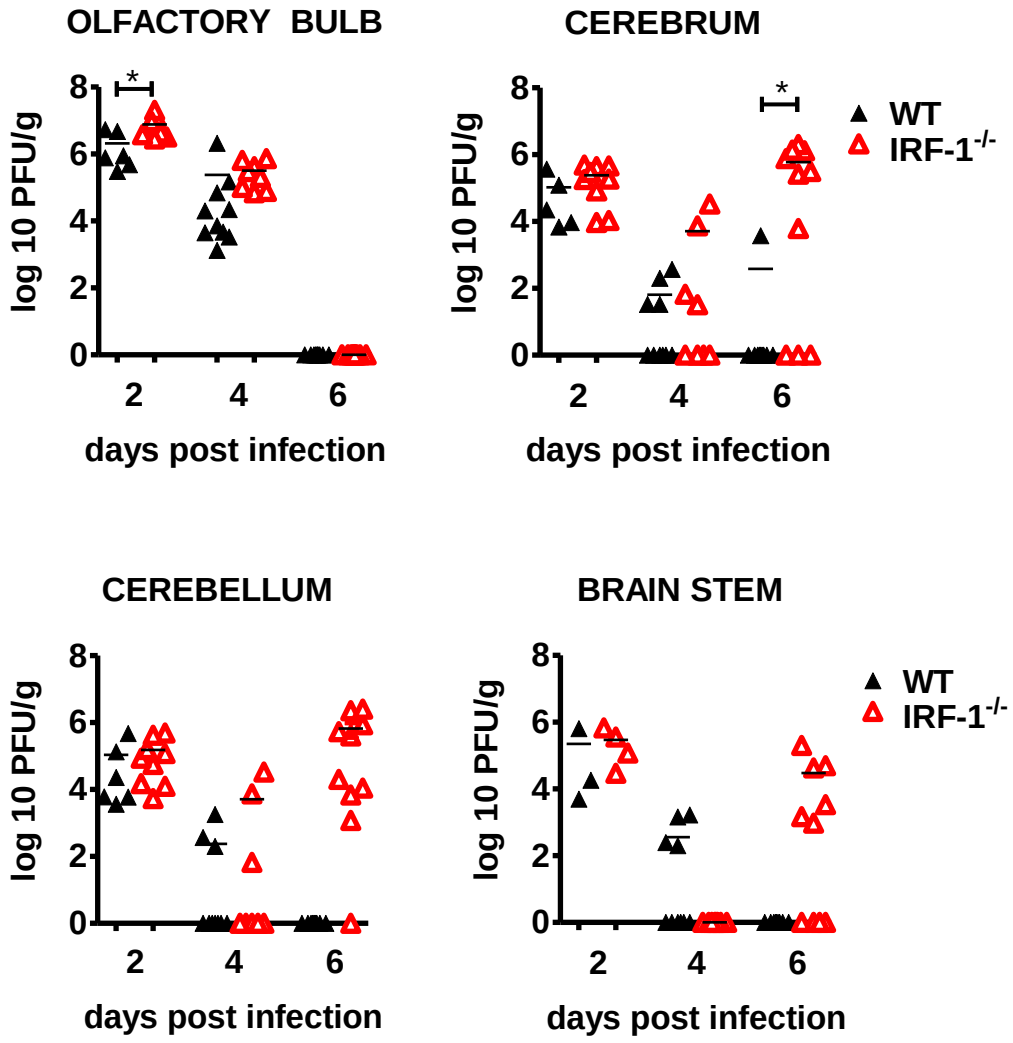

Figure 14: IRF-1 controls viral replication in the brain.

WT and IRF-$1^{-/-}$ mice were infected intranasally with 5 x 10^6 pfu of VSV. Viral burden was quantitated by plaque assay from brain parts- olfactory bulb, cerebrum, cerebellum and brain stem. Data are representative of at least two independent experiments.
Asterisks indicate statistical significance calculated by Mann-Whitney test, * $p<0.05$.

4.10 IRF-1 prevents spread of the virus

To support the contention that IRF 1 mediates protection specifically in the brain and the increased CNS virus titers in the absence of IRF-1 are due to more effective spread, we perform immunohistological analysis on infected brains of WT and IRF-$1^{-/-}$ mice at early and late time points. To track the differences of viral spread within the brain regions of WT and IRF-$1^{-/-}$ mice. We used a GFP labelled reporter virus (VSV-eGFP) **(Figure 15A/B)**. At early time points, 2 days post infection; no differences in the patterns of viral spread were visible between the WT and the IRF-$1^{-/-}$ mice **(Figure 15A)**. In the olfactory bulb which is the first target site for VSV, VSV-eGFP signals were detected exclusively within the glomeruli of both WT and IRF-$1^{-/-}$ mice. Within the regions of the cerebrum, only the striatum was found to be infected in the WT and the IRF-$1^{-/-}$ mice. Other regions of the cerebrum such as the internal capsule and hippocampus in IRF-$1^{-/-}$ mice showed no infection at this time point.

At day 6 post infection, high VSV-eGFP signals were detectable in the regions of the brain stem, striatum, internal capsule and hippocampus of IRF-$1^{-/-}$ mice. In contrast, no virus was detectable in brains of infected WT mice at this time point **(Figure 15B).** This data indicates that in the absence of IRF-1, VSV is able to spread to different regions within the cerebrum and other parts of the brain. Interestingly, high VSV-eGFP was detectable in neuron axonal fibers of the internal capsule. This data indicates that IRF-1 helps control viral spread to other vital brain regions which are important for the survival of the mice. In addition IRF-1 plays a minor role during the early phase of viral brain infection and clearance. However, IRF-1 is crucial in the control of a second phase of viral replication and spread in the cerebellum, cerebrum and brain-stem.

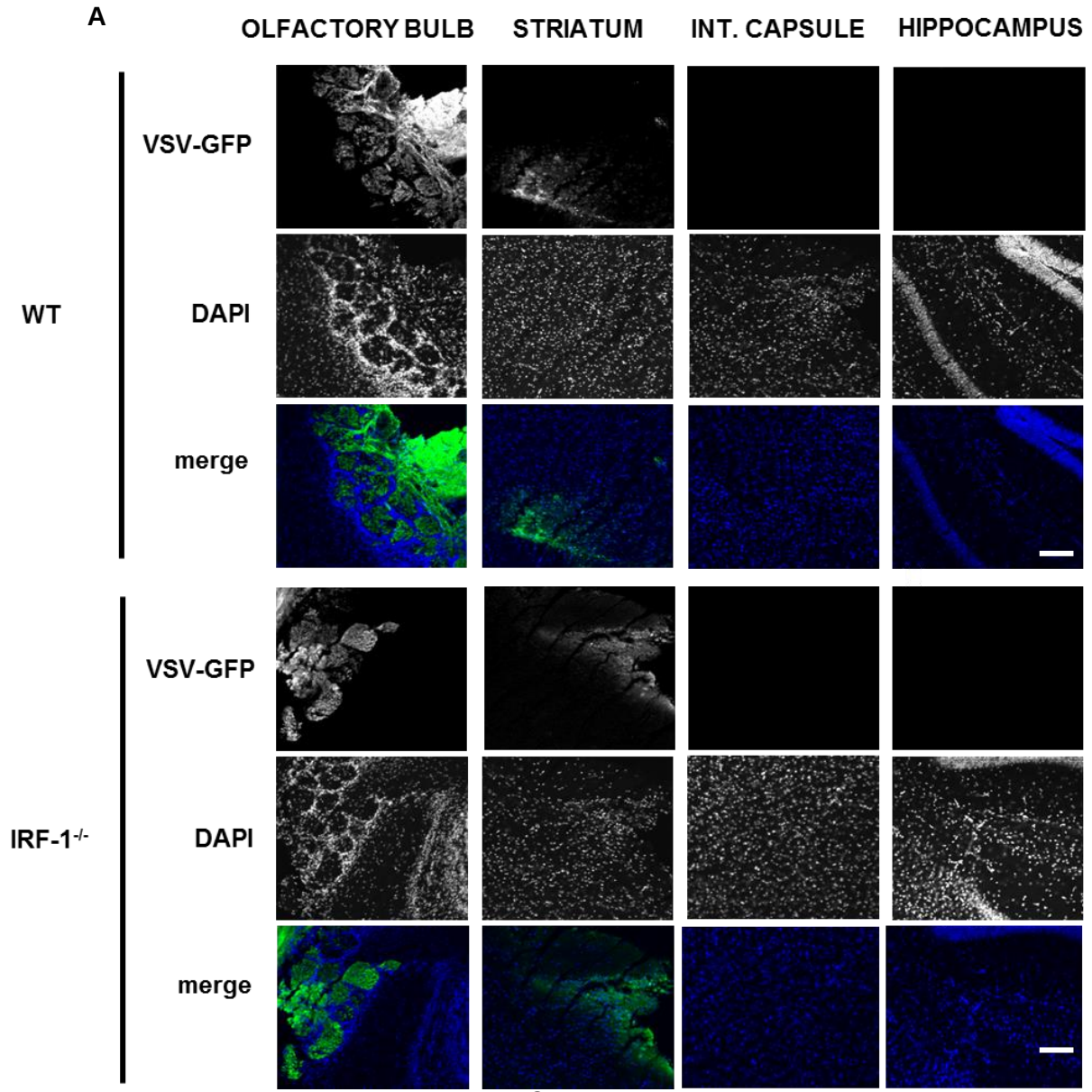
A
OLFACTORY BULB
STRIATUM
INT. CAPSULE
HIPPOCAMPUS
WT
VSV-GFP
DAPI
merge
IRF-1-/-
VSV-GFP
DAPI
merge

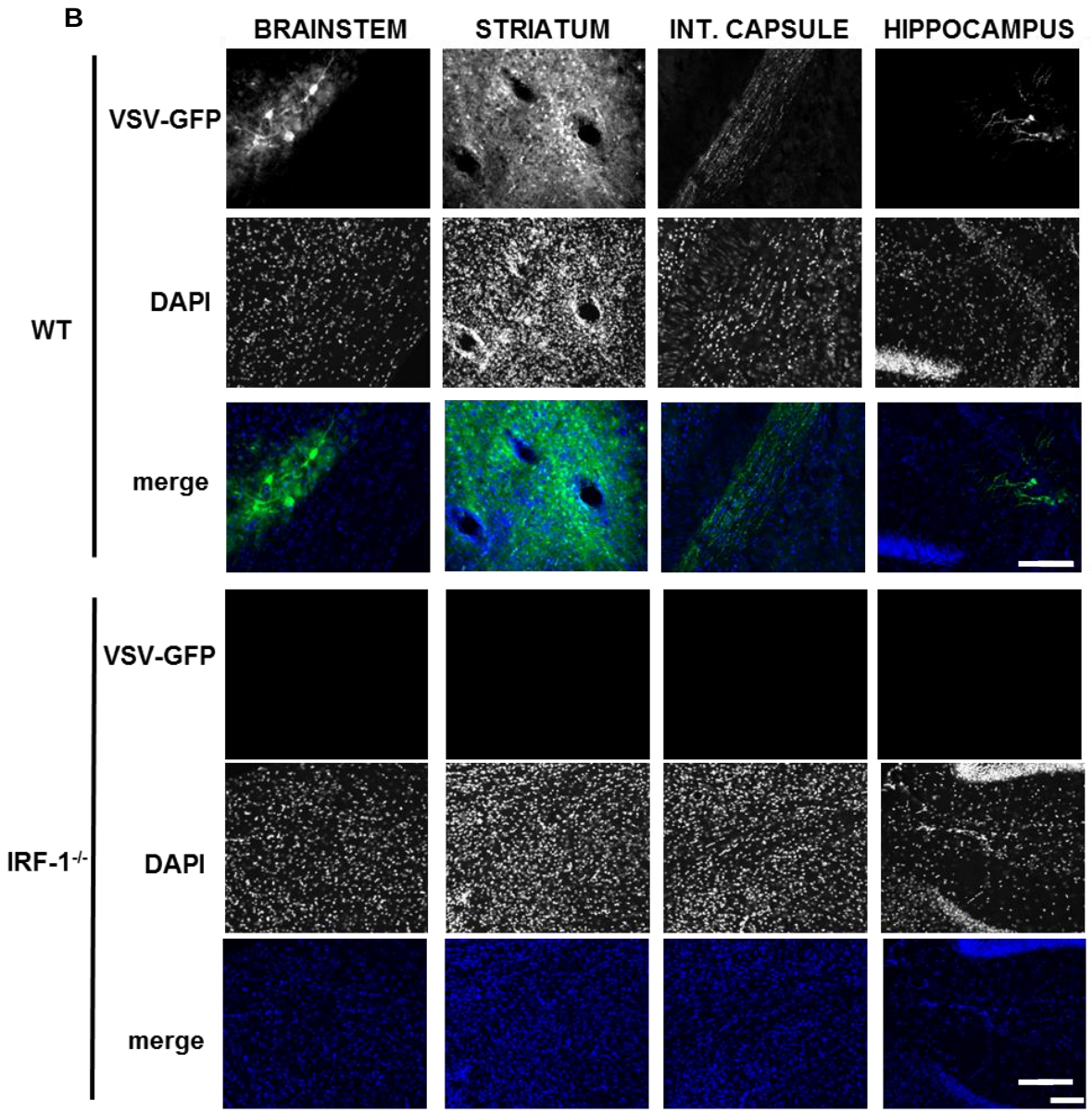
B
BRAINSTEM
STRIATUM
INT. CAPSULE
HIPPOCAMPUS
WT
VSV-GFP
DAPI
merge
IRF-1-/-
VSV-GFP
DAPI
merge

Figure 15: IRF-1 prevents viral spread in the brain.

WT and IRF-$1^{-/-}$ mice were infected with $5x10^6$ pfu of VSVeGFP. Immunohistological analysis of VSV-eGFP in the olfactory bulb, brain stem and different parts of the cerebrum (striatum, internal capsule and hippocampus) at A, 2 days post infection and B, 6 days post infections, merge: VSV-eGFP (green), DAPI (blue). Scale bar is 100 µm

4.11 IRF-1 mediates an antiviral activity that inhibits a secondary wave of virus propagation that cannot be controlled by the action of IFN-β

To dissect the different roles of type I IFN and IRF-1 during VSV infection in the brain, we determined IFN-β mRNA expression in different brain parts after i.n. infection with VSV by quantitative RT-PCR **(Figure 16)**. Interestingly, the IFN-β mRNA expression pattern and kinetics differed within the various brain regions. In the olfactory bulb IFN-β expression were detectable 2 days post infection, and its expression level declined to basal levels by day 4. No difference in IFN-β mRNA expression level was detectable between WT and IRF-$1^{-/-}$ mice. These data correlate to the kinetics of viral load where IRF-1 has no impact in the control of viral replication in the olfactory bulb.

In the cerebrum and cerebellum of IRF-$1^{-/-}$ mice, a resurgence of IFN-β mRNA induction was observed at day 6 post infection, which correlated to higher viral replication in the absence of IRF-1. The kinetics of IFN-β expression levels within the cerebrum and cerebellum indicated little if any IFN-β mRNA was produced at day 2 post infection. However, significant amounts of IFN-β were found only in the cerebrum and cerebellum of IRF-$1^{-/-}$ mice, 6 days post infection. These data indicate that loss of IRF-1 leads to higher viral replication in the late phase of virus infection, although IFN-β is expressed and corresponds well to the kinetic of enhanced viral replication in IRF-$1^{-/-}$ mice in the late phase. Thus, in both brain parts, cerebellum and cerebrum, loss of IRF-1 leads to higher viral replication in the later phase of infection in the presence of IFN-β, indicating its non-redundant function of type I IFN and IRF-1 in mediating antiviral activity.

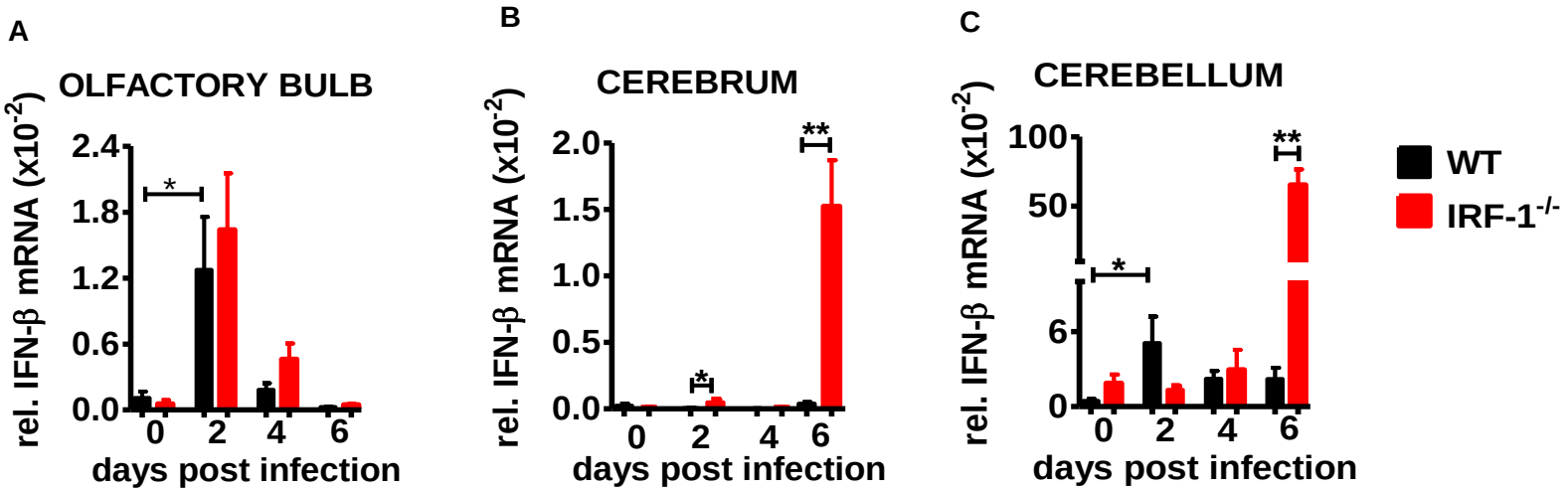

Figure 16: Type I IFN response in the IRF-1$^{-/-}$ mice is not compromised.

WT and IRF-1$^{-/-}$ mice were infected i.n. with 5 x 10^6 pfu of VSV. Expression level of IFN-β mRNA in different brain parts i.e. A, olfactory bulb, B, cerebrum and C, cerebellum was determined by real-time RT-PCR.

4.12 ISG responses are not influenced by the loss of IRF-1

IRF-1 directly induces antiviral IFN stimulated genes independent of type I IFN [42]. To define the antiviral status of the brain we investigated the induction of several prominent interferon stimulated genes (ISGs) within the cerebrum where high viral replication was observed **(Figure 17A/B/C/D)**. Increased RNA expression levels of the ISGs Mx2, Rsad2, and USP-18 mRNA were found in both WT and IRF-1$^{-/-}$ 2 days post infection, followed by a decline. However, expression levels increased again on day 6 post infection in IRF-1$^{-/-}$ mice, which correlates to IFN-β induction. IFIT-2 mRNA, which has been previously defined as an ISG to restrict VSV replication in the brain [118], was induced only at day 6 post infection. Interestingly, an increase of ISG expression in the cerebrum was also detectable in WT mice in the absence of detectable amounts of IFN-β mRNA. From this we suggest, that induction of these tested ISGs in the absence of IFN-β could be IRF-1 dependent.

Immunohistological analysis showed that IFIT-2 is expressed in brains of both, WT and IRF-1$^{-/-}$ mice, although VSV infection is not detectable in WT mice **(Figure 17E)**. IFIT-2 expression is only detectable in non-infected cells of WT animals. In contrast, in IRF-1$^{-/-}$ mice VSV positive and negative cells expressed IFIT-2. Collectively, these data suggest two waves of antiviral response in the brain after i.n. VSV infection. While the first wave of antiviral responses peaking at day 2 is IFN-dependent and induces long lasting ISG expression, the second wave is IRF-1 dependent and limits viral replication and spread.

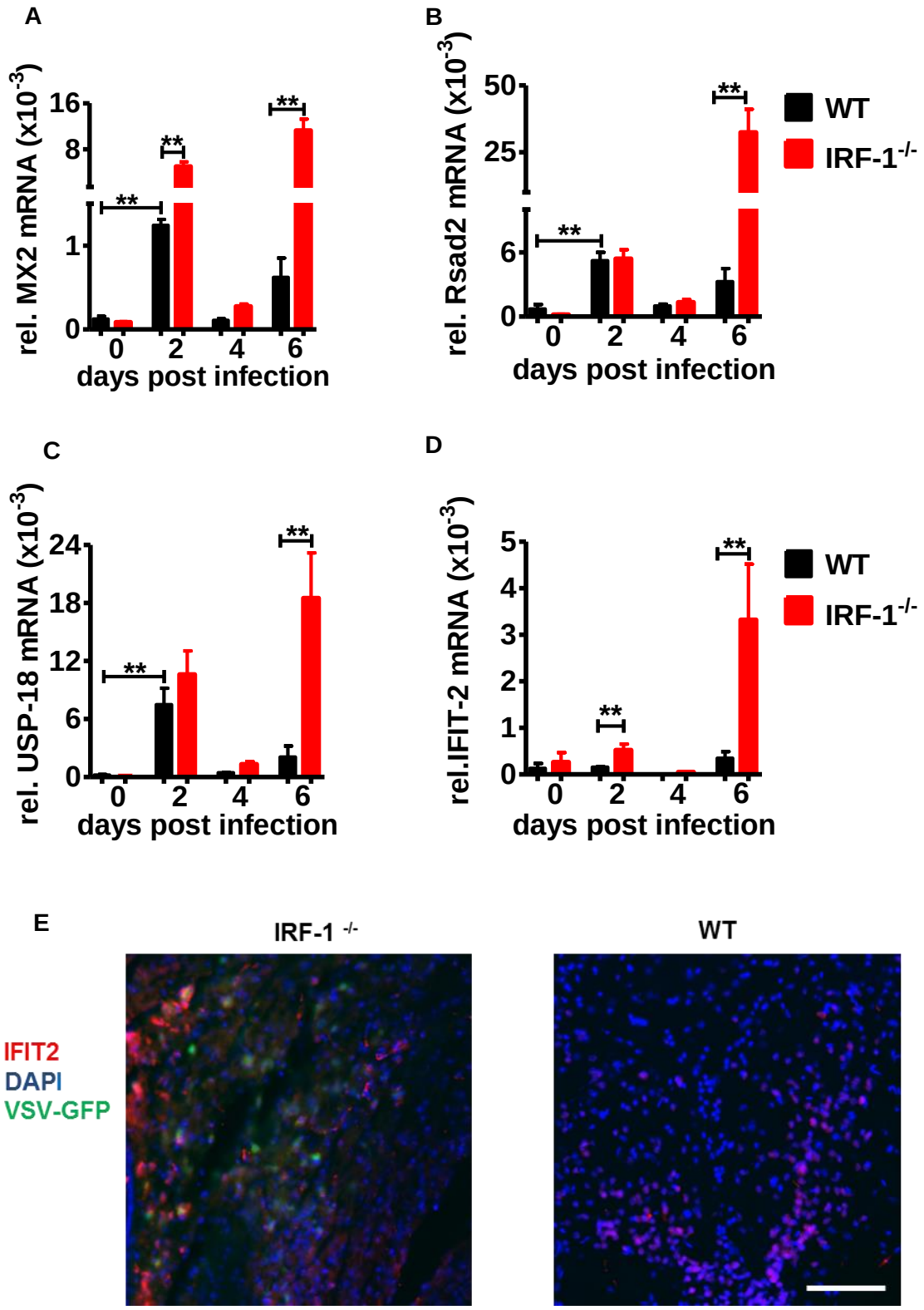
A
rel. MX2 mRNA (x10-3)
16
8
1
0
**
**
**
0
2
4
6
days post infection
B
rel. Rsad2 mRNA (x10-3)
50
25
6
0
**
**
0
2
4
6
days post infection
WT
IRF-1-/-
C
rel. USP-18 mRNA (x10-3)
24
18
12
6
0
**
**
0
2
4
6
days post infection
D
rel.IFIT-2 mRNA (x10-3)
5
4
3
2
1
0
**
**
0
2
4
6
days post infection
WT
IRF-1-/-
E
IRF-1 -/-
WT
IFIT2
DAPI
VSV-GFP

Figure 17: Type I IFN response in the IRF-1$^{-/-}$ mice are not compromised.

Mice were infected intranasally with 5 x 10^6 pfu of VSV. A/B/C/D, mRNA expression level of ISGs MX2, Rsad2, USP-18 and IFIT-2 from cerebrum was determined by real-time RT-PCR. Data represents mean with SEM of 3-7 mice in each group per time point. Asterisks indicate statistical significance calculated by Mann-Whitney test, ** $p<0.005$, * $p<0.05$.E, Immunohistological analysis of VSV-eGFP and IFIT-2 protein 6 days post infection in the cerebrum of IRF-1$^{-/-}$ mice. IFIT2 (red), DAPI (blue), VSV-eGFP (green). Scale bar is 50µm.

4.13 Brain specific induction of IRF-1

To confirm our hypothesis we determined IRF-1 expression in peripheral organs and the different brain parts of WT mice during the course of infection **(Figure 18)**. Although high viral replication was found in the lung at early time points, IRF-1 mRNA expression was not detectable in the lungs at any time point post infection, suggesting that it does not play a role in this tissue. In contrast, IRF-1 mRNA was expressed in all the regions of the brain, albeit with different kinetics. In the olfactory bulb, IRF-1 mRNA was induced strongly 2 days post infection and remained abundant until day 6. In the cerebrum, IRF-1 was induced only 6 days post infection, whereas in the cerebellum, IRF-1 was induced 2 days post infection, declined on day 4 and then remained induced until day 6. These data showed that induction of IRF-1 was tissue and time point specific and could be crucial for survival against VSV induced neuropathogenesis.

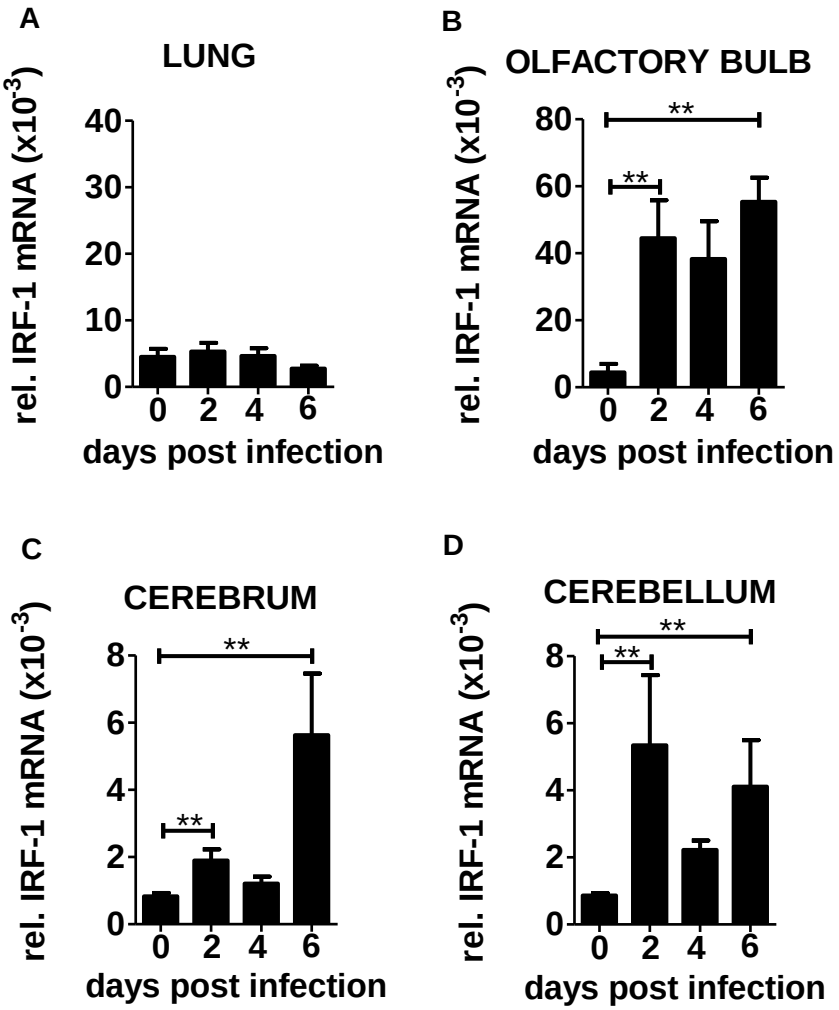

Figure 18: IRF-1 is induced at later states during VSV infection in the brain

WT mice were infected i.n. with 5 x 10^6 pfu of VSV. Expression level of IRF-1 in A, lung and B/C/D, in different brain parts were determined by real-time RT-PCR.
Asterisks indicate statistical significance calculated by Mann-Whitney test, ** $p<0.005$.

4.14 IRF-1 is induced by type I IFN independent mechanisms

IRF-1 has previously been described to be capable of being induced independent of type I IFN [42,86]. To investigate if IRF-1 induction mechanism was mediated by the type I IFNs in the brain, we used IFNAR$^{fl/fl}$NesCre$^{+/-}$ mice which lack IFNAR signalling in neuroectodermal cells. We made use of this system because IFNAR$^{-/-}$ mice die within 2 days **(Figure 1)** and hence the time points post infection was not long enough the IRF-1 mediated antiviral response which usually comes 5-6 days post infection. The IFNAR$^{fl/fl}$NesCre$^{+/-}$ mice on the other hand survives long enough to investigate the second wave of antiviral response **(Figure 7)**. A strong induction of IRF-1 mRNA was detectable within different brain parts upon intranasal VSV infection **(Figure 19).** Thus we conclude that IRF-1 is induced in the brain by type I IFN independent mechanisms.

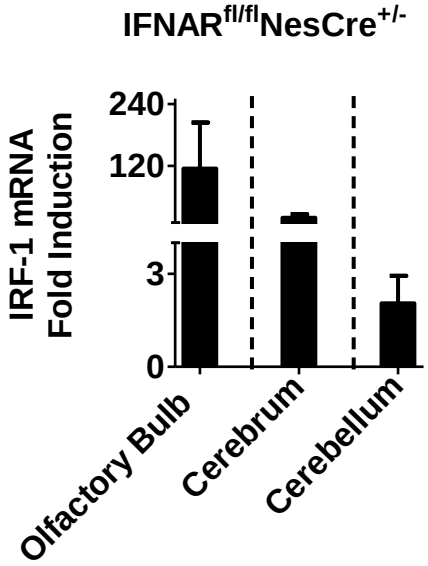

Figure 19: IRF-1 is induced by type I IFN independent mechanism.

IFNAR$^{fl/fl}$NesCre$^{+/-}$ mice was infected i.n. with 5 x 10^6 pfu of VSV. Data represents fold induction of IRF-1 in the brains parts at 6 days post infection calculated over expression levels of IRF-1 in uninfected mice.

4.15 IRF-1 is induced by type III IFN independent mechanisms

The type III IFN signals through a receptor distinct from that of type I IFN but triggers the same signal transduction pathway downstream of the receptor and induces antiviral response[119]. To check if IL-28 also known as IFN-λ is induced in the brain after VSV infection, we measured the presence of IL-28 and its receptor IL28R in the cerebrums of both WT and IRF-1$^{-/-}$ mice by quantitative RT-PCR. Consistent with previous reports that states that IL-28 is very poorly expressed in the CNS in response to a variety of virus[120], expression of IL-28 as well as the IL-28 receptor were below detection limits **(Figure 20A/B)**. In contrast, lung samples from 4 day post infected mice were used as positive controls for IL-28 and IL-28R detection and showed high expression levels. Thus, our data suggest that IRF-1 and ISG expression in the brain can be induced independent of type III IFN- and that both the type I IFN and the IRF-1 mediated antiviral effects are essential to restrict VSV induced neuropathogenesis.

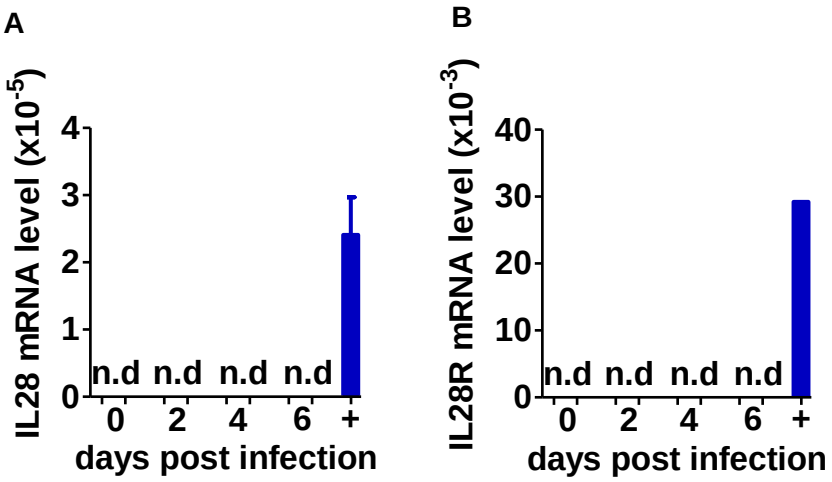

Figure 20: IRF-1 is induced by type I and Type III IFN independent mechanism.

WT and IRF-1$^{-/-}$ mice were infected i.n. with 5 x 10^6 pfu of VSV. mRNA expression of A, IL28 and B, IL28R from the cerebrum of WT and IRF-1$^{-/-}$ mice. Positive controls (+) included lung samples of VSV infected WT mice from day 4 post infection.

4.16 i.n. VSV infection leads to strong production of IFN-γ in the CNS of IRF-1$^{-/-}$ mice but not in WT mice

IRF-1 is known to be strongly induced by IFN-γ by the activation of STAT1 [121]. Thus we investigated if the induction of IRF-1 in the brain resident cells was mediated by IFN-γ secreted by the lymphocytes. We first determined the kinetic of IFN-γ mRNA expression levels in the brains of infected WT and IRF-1$^{-/-}$ mice **(Figure 21 A/B/C)**. In the olfactory bulb, no IFN-γ mRNA was induced in both WT and IRF-1$^{-/-}$ mice. In the cerebrum and cerebellum little or no IFN-γ mRNA was induced at any time point in the WT mice. In contrast to WT mice, IRF-1$^{-/-}$ mice induced very large amounts of IFN-γ 6 days post infection. This data supports the previously reported hypothesis that IRF-1$^{-/-}$ CD8^{+} T cells undergo a rapid expansion of antigen specific T cells compared to their WT counterparts. Therefore, although the CNS of IRF-1$^{-/-}$ have lower numbers of CD8^{+} T cells, the antigen specificity of these cells are higher than those of their WT counterparts. This explains why higher levels of IFN-γ are found in the CNS.

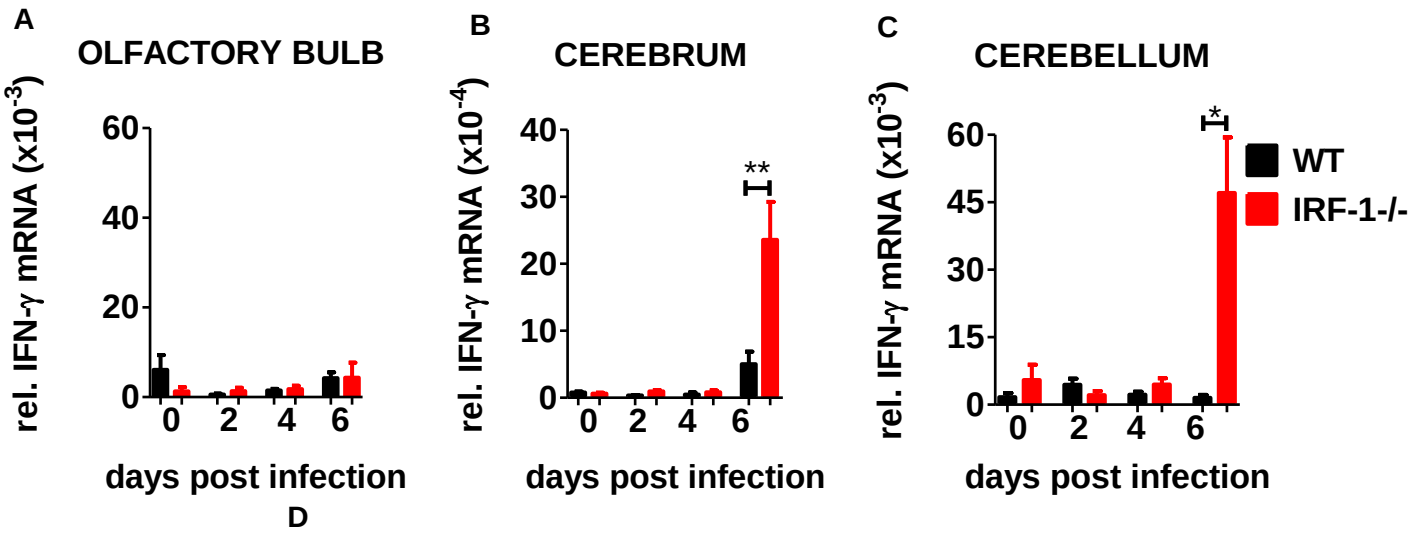

Figure 21: High levels of IFN-γ can be detected in the brains of IRF-1 mice.

A/B/C, WT and IRF-$1^{-/-}$ mice were infected i.n. with 5 x 10^6 pfu of VSV. mRNA expression of IFN-γ were quantitated from different brain parts i.e. A, olfactory bulb, B, cerebrum and C, cerebellum. Asterisks indicate statistical significance calculated by Mann-Whitney test, ** $p<0.005$, * $p<0.05$

4.17 IRF-1 is induced by type II IFN independent mechanisms

Since we detected a marginal but non-significant increase of the type II IFN i.e. IFN-γ, we investigated if the induction of IRF-1 in the brain resident cells was contributed by IFN-γ producing cells. IFN-γ expression in the CNS has been known to be attributed by infiltrating NK cells and antigen specific T cells. Since no NK cells were found infiltrating the brains of infected both WT and IRF-$1^{-/-}$ mice, we excluded the possibility of NK cells being mediators of IRF-1 induction the brain **(Figure 22A)**. Although T cells were found to be infiltrating the infected brains of WT mice, we argued that these cells were not antigen specific because IFN-γ was very poorly induced in the brain post infection **(Figure 21)**. To further corroborate our hypothesis that IRF-1 is induced by type II IFN independent mechanisms in the brain, Rag$2^{-/-}$ mice, which lack T cells were infected i.n. with VSV. All the regions of the brain tested i.e. the olfactory bulb, cerebrum and the cerebellum showed IRF-1 mRNA induction 6 days post infection albeit to different levels **(Figure 22B)**. Hence we conclude that the type II IFN producing cells types that are in usually thought to play a role in CNS infection do not play a role in the induction of IRF-1 in the brain resident cells during i.n. VSV infections.

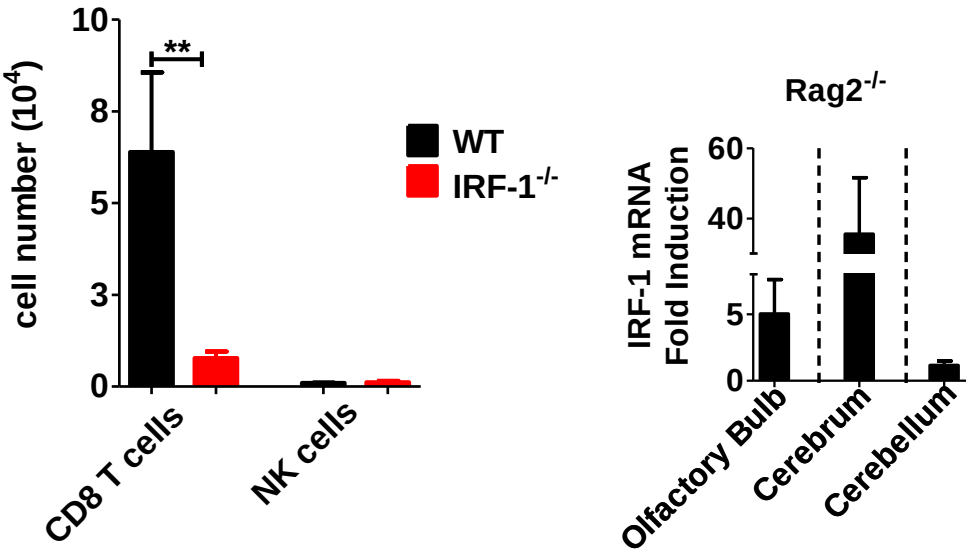

Figure 22: IRF-1 is induced by typed II IFN independent mechanism in the brain

A, WT and IRF-$1^{-/-}$ mice were infected i.n. with 5 x 10^6 pfu of VSV. Leukocytes isolated from brains of WT and IRF-$1^{-/-}$ 6 days post infection by Percoll gradient centrifugation, stained for $CD8^+$ T cells ($CD3^+CD8^+$) and NK cells ($DX5^+CD3^-$) were evaluated. Asterisks indicate statistical significance calculated by Mann-Whitney test, ** $p<0.005$. B, $Rag^{-/-}$ mice was infected with 5x10^6 pfu of VSV. mRNA expression of IRF-1 in $Rag2^{-/-}$. Data represents fold induction of IRF-1in the brains parts at 6 days post infection calculated over expression levels of IRF-1 in uninfected mice.

4.18 IRF-1 dependent antiviral mechanisms are driven by innate immune mechanisms in neurons

The primary target for VSV replication in the brain has been reported to be the neurons [108,118]. To assess if the source of the antiviral responses were governed by innate immune mechanisms, we monitored the viral replication kinetics in primary hippocampal cultures prepared from WT and IRF-$1^{-/-}$ mice **(Figure 21)**. Immunofluorescence analysis revealed that VSV could infect only

the neurons of these cultures **(Figure 21A)**. In addition, determination of viral titres in the cultures revealed a two-fold higher viral titre in IRF-1$^{-/-}$ cells compared to WT cells **(Figure 21B)**. This data shows that neurons possessed an inherent IRF-1 dependent antiviral mechanism to defend against VSV infection.

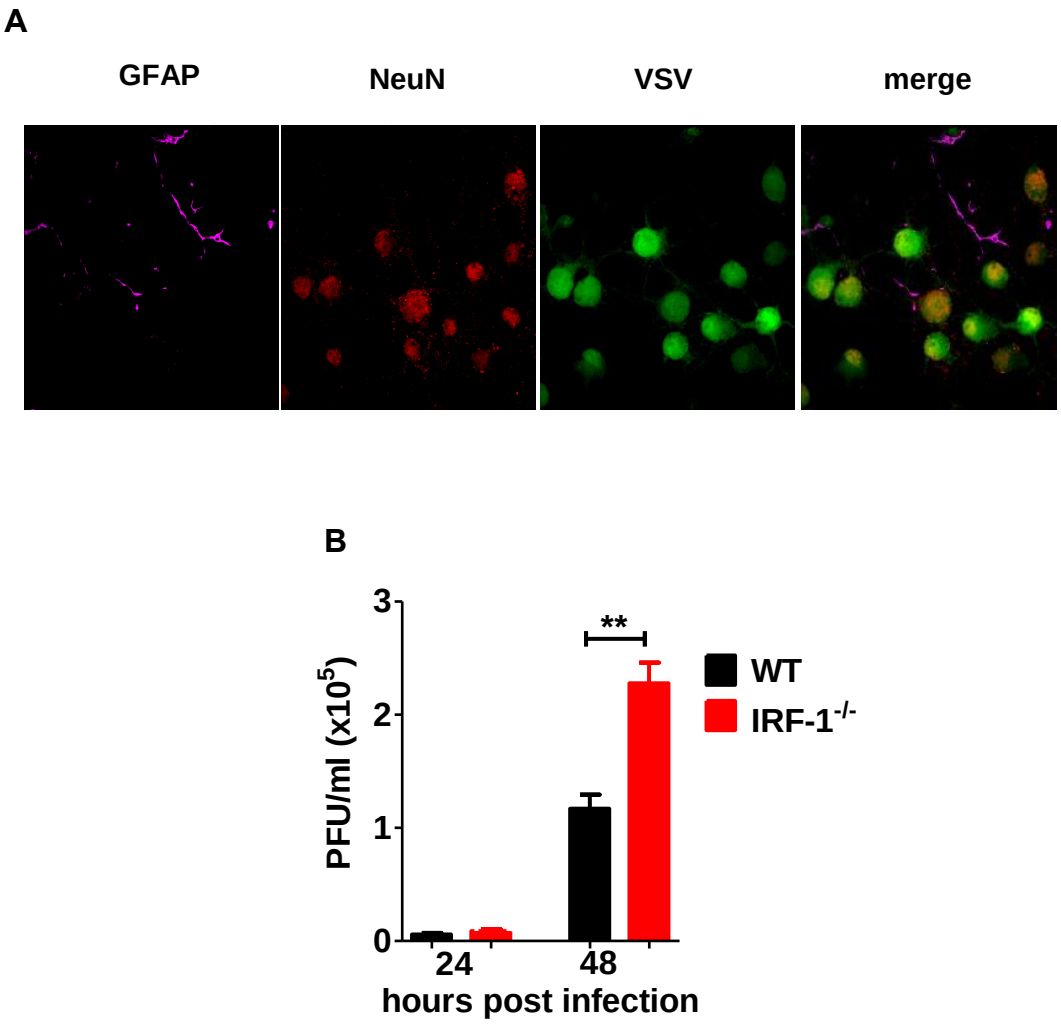

Figure 23: IRF-1$^{-/-}$ neurons are more susceptible to VSV than WT neurons

A/B Primary hippocampal neurons were cultured from WT and IRF-1$^{-/-}$ mice. A, WT neurons were infected with 0,01 MOI VSV-eGFP. 24 hours post infection; cultures were stained with GFAP (astrocytes) and NeuN (neurons) by immunofluorescence assay. B, WT and IRF-1$^{-/-}$ neurons were infected with 0.001 MOI VSV and viral replication from 24-48 hours were measured by plaque assay.
Asterisks indicate statistical significance calculated by Mann-Whitney test, ** $p<0.005$.

4.19 Loss of IRF-1 does not change the tropism of the virus

Viral infection experiments showed that IRF-1 limit viral replication specifically in neurons in vitro. To address whether the increased CNS virus titers in the absence of IRF1 in vivo are just due to more efficient viral spread in the brain or also due to a change in cell tropism we performed immunohistological analysis of 6 days post infected IRF-1$^{-/-}$ brains. The data revealed an effective infection of VSV-eGFP in neurons, whereas most of the astrocytes and all microglia remain uninfected. Interestingly, some of the microglia was associated with infected cells **(Figure 12)**. This confirmed that neurons possess an inherent IRF-1 dependent antiviral mechanism to defend against VSV infection.

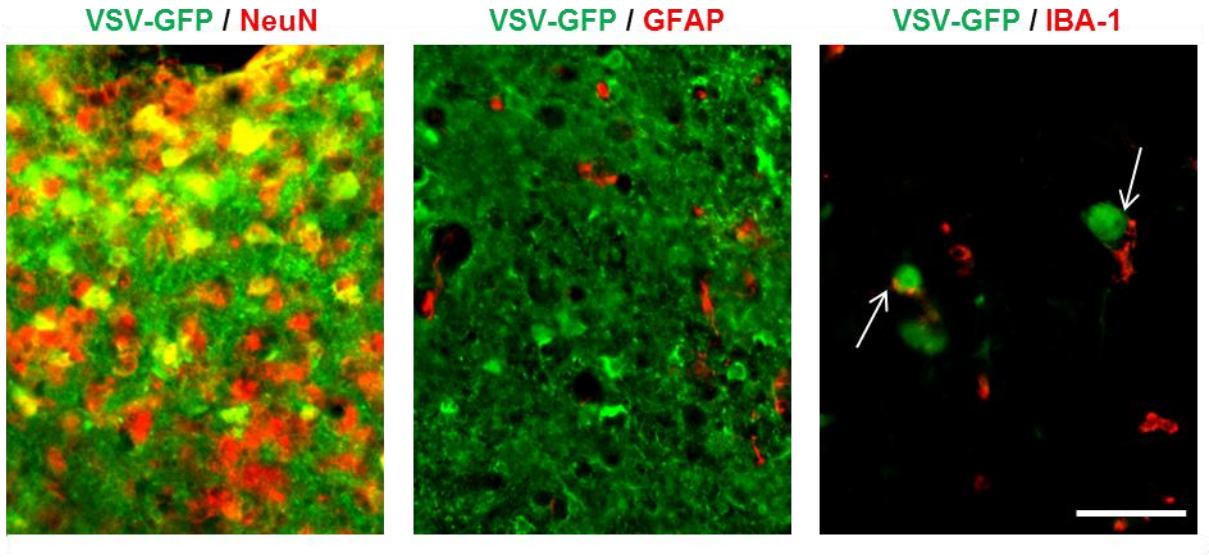

Figure 24: IRF-1$^{-/-}$ mice were infected i.n. with 5 x 10^{6} pfu VSV.

Immunohistological analysis of VSV-eGFP (green) in neurons (NeuN: red), astrocytes (GFAP: red) of the cerebrum and microglia (IBA: red) from the brain stem 6 days post infection.
Scale bar is 50µm

4.20 IRF-1 mediates antiviral responses in the brain

The CNS is typically regarded as an immune privilege site because peripheral immune cells are generally blocked by the blood brain barrier (BBB). However, neuroinflammation can be initiated in response to a pathogenic attack. Inflammation is associated with the breakdown of the BBB and attraction of several inflammatory cells to the target site. Since, infected IRF-$1^{-/-}$ mice have enhanced viral replication in their brain and succumb with symptoms of fatal encephalitis, we characterised the extent of the inflammatory response in WT and IRF-$1^{-/-}$ mice post i.n. VSV infection **(Figure 25A/B)**. Higher numbers of infiltrating monocytes characterised by CD45Hi CD11b+ expression level were quantitated in the knockout mice compared to their WT counterparts 6 days post infection. At this time point higher numbers of activated microglia characterised by the CD45LoCD11b+ expression levels were also detectable the IRF-$1^{-/-}$ mice. These results suggested that IRF-$1^{-/-}$ mice had more severe inflammatory responses in the brain.

One of the characteristics of neuroinflammation is the secretion of proinflammatory cytokines by the immune cells in the brain. To support the hypothesis that IRF-$1^{-/-}$ mice experience a more severe inflammatory response than their WT counterparts, we measured mRNA levels of proinflammatory cytokines IL-1ß and TNF-α from the cerebrum **(Figure 25C/D)**. The mRNA expression of both cytokines was increased in the IRF-$1^{-/-}$ cerebral tissues. These data suggest that higher replication of VSV by the loss IRF-1 leads to enhanced inflammatory response which could contribute to encephalitis leading up to neurotoxicity and death.

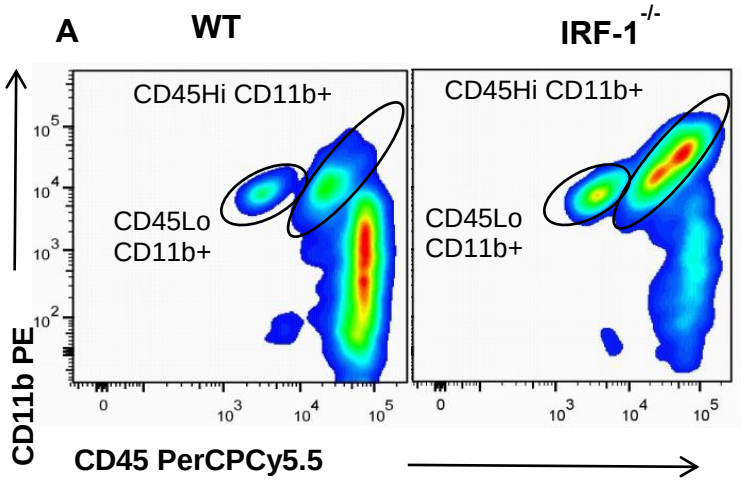
A
WT
IRF-1-/-
CD45Hi CD11b+
CD45Lo
CD11b+
CD45Hi CD11b+
CD45Lo
CD11b+
CD11b PE
CD45 PerCPCy5.5

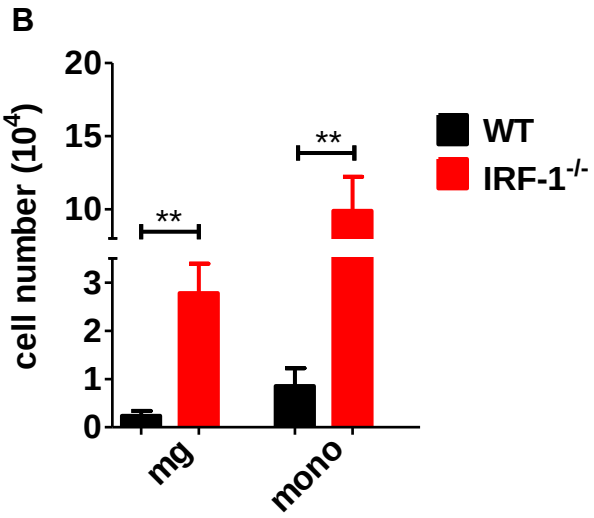
B
cell number (10^4)
20
15
10
3
2
1
0
**
**
WT
IRF-1-/-
mg
mono

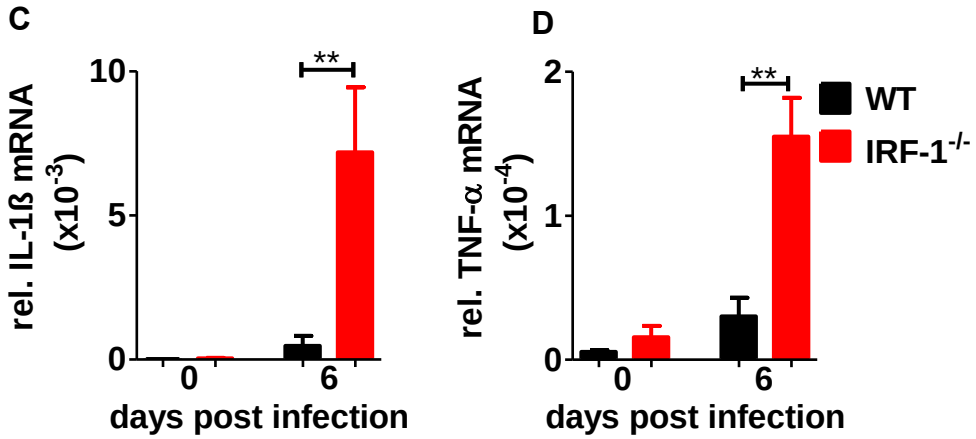

Figure 25: The absence of IRF-1 leads to an inflammatory response in the brain

WT and IRF-1$^{-/-}$ mice were infected intranasally with 5 x 10^6 pfu VSV. A/B, Leukocytes were isolated from brains of WT and IRF-1$^{-/-}$ 6 days post infection by Percoll gradient centrifugation, stained for CD11b and CD45, and analyzed by flow cytometry, A, Representative flow cytometry profiles of CD11b and CD45 staining of brain leukocytes from WT and IRF-1$^{-/-}$ mice are shown, B, Total cell numbers for infiltrating monocytes (mono) (CD45Hi CD11b+), microglia (mg) (CD45Lo CD11b+) CD8$^+$ T cells (CD8$^+$) and NK cells (DX5$^+$CD3$^-$) were evaluated. C/D, Expression levels of IL-1ß and TNF-α mRNA were recorded by real-time RT-PCR from the cerebrum of WT and IRF-1$^{-/-}$ mice.
Asterisks indicate statistical significance calculated by Mann- Whitney test, ** $p<0.005$, * $p<0.05$.

5 DISCUSSION

The central nervous system (CNS) harbours highly differentiated cells, such as neurons that are essential to coordinate the functions of complex organisms. Numerous cell types act in accord to maintain its integrity and its functions, separated into three main groups: neurons, the glia, and endothelial cells. This organ is partly protected by the blood-brain barrier (BBB) from toxic substances and pathogens carried in the bloodstream. For decades, the immune privilege of the CNS was understood as an absence of an immune system inside the CNS, and the BBB was considered only as a barrier isolating the CNS from the peripheral immune system, preventing the entry of infectious agents and immune cells into the CNS [96]. Extensive work in the last decade unravelled the presence of a specialised intrinsic innate immune system in the CNS.

5.1 Role of IRF-1 in antiviral responses in the CNS

The innate immune system is essential to limit viral replication before adaptive immunity is stimulated. The engagement of viral PAMPs on TLRs and RLRs are known to drive IFN-β mediated antiviral responses while NLRs are known to drive antiviral responses mediated by IL-1β. Both type I IFN and IL-1β mediated responses have shown to play important innate responses in the CNS against neurotropic viruses. In this study, using VSV as a model for neurotropic infections we report IRF-1 as an essential regulator of host innate antiviral response that is not involved in rapid IFN induction.

The susceptibility of IRF-1$^{-/-}$ mice to VSV depends on the route of infection. While IRF-1$^{-/-}$ mice succumb to i.n. VSV infection at a sub-lethal dose, all mice survive the infection by the i.v. route. This could be due to the fact that this transcription factor plays a non-redundant role in certain cell types. Upon intranasal infection, VSV infects olfactory receptor neurons and is transported to the olfactory bulb via the olfactory nerves, from where the virus spreads trans-synaptically to other regions of the brain [92]. However, upon i.v. VSV infection, virus replication is restricted to the periphery. Unlike other members of the IRF family such as IRF-3 and IRF-7, IRF-1 does not need to undergo post-translational modifications to become active. IRF-1 instead needs to be induced to carry out its antiviral activities. Our results show that i.n. VSV leads to IRF-1 induction in the CNS but not in the periphery. Hence, IRF-1 is a crucial transcription factor driving antiviral activities in special cells of the CNS.

5.2 Antiviral action of IRF-1 against VSV

Although IRF-1 was originally identified as an IFN inducer upon virus infection [36,122,123], the antiviral effect of IRF-1 was not due to a hampered type I IFN response. Instead, other members of the IRF-family such as IRF-3 and IRF-7 have been identified as regulators for type I IFN expression [54,66]. Mechanistically, IRF-1 and type I IFN are known to induce partially overlapping sets of ISGs that show broad antiviral activity against a range of viruses, but several studies have shown specific genes to be mediated directly by IRF-1 [87,124]. Detailed analysis of the viral titres from different brain regions revealed a temporal role of IRF-1 in the control of viral replication. While type I IFN plays a critical role in early stages of infection, IRF-1 is essential in limiting viral replication at later stages. Our data also suggests that while the IFN mediated antiviral effects might be driven by the olfactory bulb, IRF-1 mediated antiviral are redundant in the olfactory bulb at any time point. Instead, other regions of

the brain i.e. the cerebrum, cerebellum and the brain stem are dependent on the IRF-1 mediated antiviral mechanisms to defend against the virus at the late stages of infection. Moreover, analysis of viral titres as well as the kinetics of IFN-β in the different brain parts suggested an IFN-independent antiviral response by IRF-1.

Previous in-vitro studies identified that IRF-1 could induce antiviral mechanisms in the absence of type I IFN signalling. To confirm if such a mechanism could exist in the CNS, infection experiments with IRF-$1^{-/-}$ NesCre$^{+/-}$IFNAR$^{fl/fl}$ and IRF-$1^{+/-}$ NesCre$^{+/-}$IFNAR$^{fl/fl}$ mice were carried out. The former succumbed earlier to the infection, indicating essential antiviral responses by IRF-1 that are overlooked due to the strong effects of type I IFN. IFIT-2 is identified as an ISG that plays a significant role against VSV in the brain. However, IFIT-2 is induced in the brain of IRF-$1^{-/-}$ mice with kinetics exactly similar to IFN-β, indicating that the effect of IRF-1 could be through a distinct group of IRF-1 regulated genes. One study demonstrated the IRF-1 mediates induction of an otherwise known ISG gbp-2 in the absence of type I IFN [125]. This demonstrates the possibility of distinct subgroups of ISGs which co-ordinate IFN dependent and independent effector functions.

5.3 Neurons hold intrinsic innate immune defences

Literature has previously described microglia as crucial immune cells of the brain. However, more recent studies have shown neurons capable of executing crucial antiviral defence mechanisms. IFNAR$^{-/-}$ neurons as well as IL-1β r$^{-/-}$ neurons show increased susceptibility to viral infection than their WT counterparts [108,126]. VSV infection in the brain leads the virus to selectively replicate in neurons [118]. We showed that the loss of IRF-1 did not change the tropism of the virus and primary hippocampal neurons isolated from IRF-$1^{-/-}$ mice showed higher VSV replication rates compared to WT control. Recently it was reported that neurons from evolutionary distinct regions of the brain

respond differently to WNV infection [127]. No impact of IRF-1 was detectable in the olfactory bulb, while all other brain regions tested showed an IRF-1 dependent decrease of viral load. This observation is also in line with VSV infection studies in primary olfactory neurons, which show no impact in IRF-1 mediated antiviral response induced by IFN-γ [128]. In the absence of IRF-1, VSV can more effectively spread to different regions of the brain such as the brain stem, the striatum, the internal capsule and the hippocampus which are crucial regions of the brain. The infection of the internal capsule, which separates caudate nucleus and the thalamus from the patatum and globus pallidus could explain how VSV is able to overcome natural barriers in the brain and infect additional regions in the brain.

Our findings indicate that the increase of viral load is not due to a broader cellular tropism and neurons are still the primary target for VSV replication and spread. However, other uninfected cell types in the vicinity of infected cells might still be involved in executing antiviral effects. Virus infection of astrocytes and microglia was reported in in vitro cultures and intranasal infection of young mice [129]. Infection of 3-4 week old mice with very high doses VSV does not reflect the same infection model as ours, because the BBB is not fully developed in mice less than 6 weeks old. However, our results indicate that the microglia is activated post i.n. VSV infection as expression of proinflammatory cytokines could be quantitated. Microglia is very commonly referred to as the “resident macrophage like cell-type” in the CNS. IRF-$1^{-/-}$ macrophages are more susceptible to VSV replication than their WT counterparts suggesting that IRF-1 has an innate role in this cell type (unpublished data).Moreover production of inducible nitric oxide synthase (iNOS) which is a potent compound against a variety of pathogens, is induced by IRF-1[41]. Hence, it is worth investigating if IRF-1 plays a role in microglia responses against VSV although these effects could be indirect as microglia were not found infected but some showed them touching infected neurons. Similarly the role of IRF-1 in astrocyte mediated responses is also worth investigating.

5.4 Role of adaptive immunity in i.n. VSV infections

Previous studies have reported the essential role of the adaptive immune response against VSV infections. Besides innate resistance mechanisms, neutralizing antibodies also control VSV replication in peripheral organs and inhibit lethal viremic spread of VSV to the CNS [130]. It has been demonstrated that IRF-$1^{-/-}$ mice display several defects in adaptive immune response, therefore an impaired response could have contributed to death of VSV-infected IRF-$1^{-/-}$ mice. We found normal VSV-neutralizing antibody response in the serum of IRF-$1^{-/-}$ mice. Although T cell responses are not crucial for VSV infections as T cell deficient mice or mice with T cell depletion showed no impact on VSV replication [131], virus-specific T cells can be found at late time points. IRF-$1^{-/-}$ mice have a blunted and dysfunctional CD8+ T cell response. However, in WNV infection $CD8^+$ T cells were fully capable of lysing target cells and clearing viral infection from neurons and the brain [132]. In VSV infected brains, lower numbers of $CD8^+$ T cells are detected. In bone marrow chimeric mice reconstituted with WT donor cells, IRF-$1^{-/-}$ and WT recipients showed a competent T cells infiltration in the infected brains. Despite this IRF-$1^{-/-}$ recipients showed no signs of improved survival. In addition, IFN-γ mRNA expression is low. Moreover, $Rag2^{-/-}$ mice could also induce IRF-1 in the different brain regions. Thus we conclude that the IRF-1 signalling in the brain resident cells is critically required to restrict virus replication.

IRF-$1^{-/-}$ mice have a defective Th1 T cell response because IRF-1 plays a role in the transcription of IL-12 and IL-12R. However, since we could establish that in the context of i.n. VSV infection, T cell responses play a minor role, it makes it an excellent model for studying innate immune responses. However, for other pathogenic challenges for which the host relies on a competent T cell response to combat the infection, IRF-$1^{-/-}$ mice are susceptible [133]. IRF-1 deficient mice show a higher susceptibility to viral infection with different viruses such as EMCV, murine γ-herpesvirus 68 or West Nile virus [132,134,135]. However, the

antiviral response of IRF-1 is pathogen specific because as infection with *Nippostrongylus brasiliensis* can be controlled in the knockout animals [46,136].

5.5 The synergistic action of IFN and IRF-1 in the CNS

The critical finding of this study is that the control of VSV infection in mice is carried out in two waves of antiviral responses **(Figure 26)**. In the first wave, the host responds to virus entry, replication and spread to the different brain parts. This response is characterized by type I IFN induction which is crucial to limit viral replication in both WT and IRF-$1^{-/-}$ mice. Thus viral titres within the different brain regions drop by day 4 post infection in both the mice but however, a complete viral clearance is not achieved. The second wave of antiviral responses which is clearly IRF-1 mediated is thus required to achieve complete clearance. IRF-$1^{-/-}$ mice shows a resurgence of viral load in the cerebrum, cerebellum and the brain stem. The function of IRF-1 is non-redundant to type I IFN activity and the slightly higher concentrations of IFN-β in IRF-$1^{-/-}$ mice are possibly induced by increased viral load but still succumb to the infection. The strict limitation of type I IFN responses to the early phase of infection could be due to its potential negative effects in CNS. Type I IFNs were recently shown to have both beneficial and detrimental effects in the central nervous system and a strict regulation is necessary to co-ordinate a tightly balanced equilibrium between cellular activation and inhibition [137]. IRF-1 could be essential to maintain that homeostasis in the brain.

5.6 Potential IRF-1 inducting mechanisms

With the exception of embryonic cells, IRF-1 is expressed in basal levels in all cell types examined. For IRF-1 activity to be executed, IRF-1 does not have to

be post-translationally be modified like IRF-3 and IRF-7 to become active. IRF-1 intrinsically activates gene expression with levels of expression determining its activity. Therefore, to have antiviral activity IRF-1 first needs to be induced. Both type I and type II IFN can induce IRF-1 but our data suggests that during i.n. VSV infections the second wave of IRF-1 mediated antiviral action is driven by an IFN independent mechanism. Insights to how and what induces IRF-1 in neurons is yet to be discovered.

IL-1β responses mediated by the inflammasome signalling have also been identified as crucial innate immune responses against neurotropic viruses such as WNV [138]. IL-1β is a known inducer of IRF-1 but this could be cell type specific [139,140]. If the inflammasome signalling Is involved in the induction of IRF-1 in the brain resident cells is also yet to be investigated.

Other possibilities for IRF-1 induction in neurons could be either direct PRR signalling events such as the involvement of MyD88 or MAVS signalling in the induction of IRF-1 or by proinflammatory cytokines such as TNF-α and IL-1. Both possibilities are equally valid as two independent studies show antiviral signalling pathway which leads to MyD88 and IRF-1 interaction following TLR activation [141,142]. Moreover, IL-1 and TNF are already known to be an inducer of IRF-1 [140].

Signalling events leading to STAT-1 phosphorylation have previously been identified as the mechanism for IFN independent IRF-1 induction in fibroblasts [42]. Therefore, it is possible that any PRR signalling event that could lead to STAT-1 activation is a potential IRF-1 inducing mechanism.

Which mechanism plays a role in inducing IRF-1 in the CNS in response to pathogenic challenges still remains un-investigated.

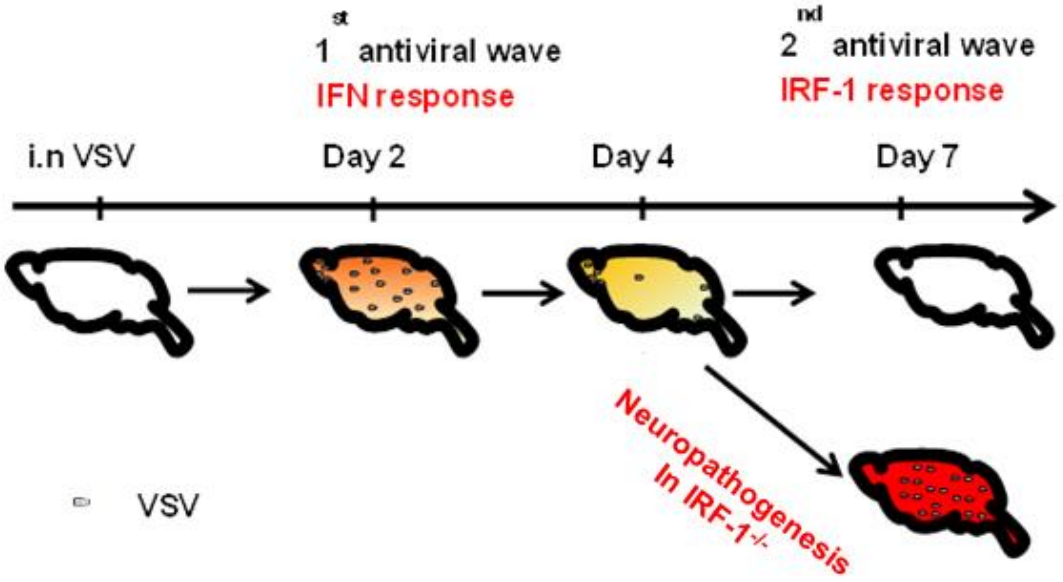

Figure 26: Model describing two waves of antiviral responses regulating defences against i.n. VSV infection.

5.7 Evolutionary perspective into IRF-1 mediated antiviral defenses

In contrast to type I IFN, IRFs are not secreted from cells indicating that an IRF-mediated antiviral response is cell intrinsic and therefore limited to infected cells. This leads us to believe that IRF mediated antiviral defence is the ancient response while the IFN mediated action has evolved to strengthen the innate immune network.

With time more viruses are finding ways to circumvent the IFN action. Therefore in future, cells would have to rely on other non-redundant antiviral mechanism to defend itself from viral attack. Hence, there is an urgent need to identify other non-redundant mechanisms for antiviral defences. Given that the IRF family is crucial for host defence immunity against pathogens, a more detailed

understanding of how the IRF system's signalling pathways are turned on and off could make the IRF family an attractive target for therapy for infectious diseases.

6 MATERIALS AND METHODS

6.1 Consumables

Table 3: List of consumables used

Article	Company
Cell culture plates (96 well, 24 well, 12 well)	Nunc, Corning
Tissue Culture dishes	Corning, Greiner Bio-one
Tissue culture flasks ($25cm^2$, $75cm^2$, $125cm^2$)	Corning, Greiner Bio-one
Flow cytometry tubes	Sarstedt
Combi tips	Eppendorf
Safe lock tubes	Eppendorf
PCR tubes	Kisker Biotech, Steinfurt
Cryovials	Corning
Reaction tubes (15ml and 50 ml)	Greiner Bio-one
Probe tubes 2ml	Omnilab
Cell strainer (40µm and 70µm)	BD Falcon

Table 4: List of equipment used

Equipment	Product Name and Manufacturer	Model
Autoclave	Belimed Dampf Sterilisator	6-6-6 HS1,FD
Cell Counter	Casy-DT 1, Schaerfe Systems	-
Cell separator	MACS Miltenyi	
Centrifuges	Eppendorf	5417C
	Heraeus Biofuge	13
	Hettich Rontana/S	-
	Cooling Centrifuges Sorvall	-
	Superspeed	RC5
	Minifuge Heraeus-Christ	-

	Heraeus Biofuge fresco Inflexible rotors Swing rotor Juan	- GSA, GS3, SS34 HB4 CR412
Deionized water	Milli-Q	
Eliza Reader	Multiskan EX reader, Thermo Electron Corporation	-
Fast Prep	MP	
Freezer	-20°C:Liebherr - 80°C: Thermo Forma	GS3183?
Fridge	Liebherr	UKS3600
Incubators for Cell Culture	Labotect	C200
In Vivo, Bioluminescence Imaging Machine	Xenogen IVIS system, Caliper	IVIS 200
Light Cycler	Roche	480
LSM	LSM Carl Zeiss Confocal	-
LSR II	BD	
Luminometer	Berthold Lumat LB	9507
Microwave	Whirlpool	Pro 825
Mini centrifuge	Heraeus Christ Minifuge GL Biofuge fresco	- -
Micropipettes	Gilson	-
Nitrogen tank	HarscoK-Series	17K
PCR Machine	T3 Thermocycler, Biometra	-
pH meter	Beckmann	M340
Photometer	Nanodrop	ND-1000
Pipettor	Pipetboy IBS Integra Biosciences	-
Power Pack	Biorad Power Pac	1000
Precision Weighing Scale	Sartorius	-
Sterile Work Benches	Steril Gard Class II Type A/B3, Baker Company. Herasafe, Heraeus	SG 400E HSP 18
Thermomixer	Eppendorf	5436, 6350
pH meter	Beckman	M340
Vortex	Scientific Industries Vortex Genie 2	-
Water Bath	GFL	-

6.2 Chemicals

The chemicals used were supplied by the following companies: Amersham Biosciences, Bayer, Biolabs, Bioline, BioRad, BRL Difco, Gibco, Merck, Promega, Qiagen, R&D systems, Roche, Seromed, Serva and Sigma.

Enzymes were purchased from Bioline, Invitrogen, Promega, Roche and oligonucleotides were synthesized at Eurofins MWG Operon.

Antibodies were purchased from eBioscience, SYSY, Sigma, Millipore and Beckton Dickenson.

6.3 Consumables

Materials for working with eukaryotic cells were purchased from companies Corning, Gibco, Sigma, Nunc.

6.4 Computer software

This thesis was written using the Microsoft (MS) Word 97-2003 version. Tables, calculations and graphs were constructed on MS Excel 97-2003 as well as Graph pad PRISM. Figure design and annotation was performed with MS PowerPoint 2010 Microscopical image analysis was performed with ImageJ (National Institutes of Health) .Flow cytometry data was acquired with LSRII (BD) and analyzed using FlowJo v7.6 . Quantitative PCR (qRT-PCR) results were analyzed and calculated using the LightCycler 480 software. Preparation of figures and statistical analysis of data was done using GraphPad Prism.

6.5 Sterilisation

Glassware was sterilized at 180˚C for 4 hours prior to use. Plastic materials such as Eppendorf tubes, pipette tips and solutions for cell culture were autoclaved at 121˚C for 25 minutes. Solutions that could not be autoclaved were filtered through a 0.22µm filter under a clean working bench.

6.6 Photometric determination of nucleic acids

Concentration of nucleic acids was assessed by measuring absorbance at A260 on a Nanodrop-1000. Purity of nucleic acids preparation was determined by the A260/280 ratio. A value appreciably lower than 1.8 and 2 for DNA and RNA respectively indicates contamination due to protein, phenol or organic compounds in the sample.

6.7 Virus

In this study, vesicular stomatitis virus (VSV) of serotype Indiana (Mudd-Summers isolate) was used. Virus production was carried out on BHK cells.

6.8 Cell culture

Cell culture work was carried out in a sterile workbench with vertical air flow. The working surface and the equipment used before and after working was disinfected with 70% ethanol. In addition, disposable consumables or autoclaved or sterile-filtered solutions or media were used. Before starting work, all solutions and media were on preheated in a 37°C water bath. Vero cells and primary neuronal cells were cultured at 37°C with 5% CO2 and 95% relative humidity.

6.8.1 DMEM (Dulbecco's Modified Media)

13,63 g/l DMEM Puder (Sigma), 3,67 g/l (44 mM) Sodium Hydregen carbonate 2,6 g/l, 10 mM HEPES, pH 7,2

6.8.2 100 x Pen / Strep

6.06 mg / ml ampicillin (10,000U/ml), 10 mg/l streptomycin, pH 7.4, stored at -20°C

6.8.3 100 x Glutamine

29.23 mg/ml glutamine, sterile filtered, stored at -20 ° C

6.8.4 Media for Vero cells

DMEM, 1 × Pen/Strep, 1 x glutamine, 10% FCS (Lonza)

6.8.5 Media for Neuronal cells

Neurobasal media (Invitrogen) supplemented with 2% B27 (Invitrogen), 2x N-2 supplement (Invitrogen), 1% Pen/Strep and 0.5 mM Glutamax.

6.8.6 Phosphate buffer saline (PBS)

140 mM NaCl, 27 mM KCl, 7.2 mM Na2HPO4, 14.7mm KH2PO4, pH 6.8-7.0

6.8.7 Gey's balanced salt solution (GBSS)

0,22 g $CaCl_2 \cdot 2H_2O$, 0.370 g KCl, 0.030 g KH_2PO_4, 0.210 g $MgCl_2 \cdot 6H2O$, 0.070 g MgSO4·7H2O, 8000 g NaCl, 0.227 g $NaHCO_3$, 0.120 g Na_2HPO_4 1000 g D-glucose in 1000ml H_2O

6.8.8 GBSS/Glucose

50ml GBSS+0.5% 50% Glucose, pH 7.2, sterile filtered.

6.8.9 TEP (trypsin EDTA)

6 mM EDTA, 0.1% trypsin (Gibco) in PBS

6.8.10 Passaging cultured cells

When cells in a flask reach 90% confluency, they should be passaged. The cells were first washed in PBS, trypsin with TEP for a few minutes. The reaction of trypsin is stopped by DMEM media which contains 10% FCS, the inactivating factor.

6.8.11 Neuronal cell isolation and infection

All the dissection tools should be sterilised in ethanol and then heat flamed 30 minutes before starting the procedure. The procedure should be carried out on ice. Primary cultures of mouse hippocampal neurons were prepared from mouse embryos E18. Embryos were decapitated and the brains were kept in ice-cold Gey's balanced salt solution supplemented with glucose **(refer 6.8.7 and 6.8.8)**. After dissection the hippocampi were isolated and then dissociated by 30 min incubation with trypsin followed by mechanical separation using a

Pasteur pipette. 70.000 Cells were seeded on poly-L-lysine coated cover slips and incubated in Neurobasal medium (Invitrogen) supplemented with 2% B27 (Invitrogen), 2 x N-2 supplement (Invitrogen) and 0.5 mM Glutamax at 37°C, 5% CO2 and 99% humidity. After 3 weeks, cells were infected with either VSV or VSV-eGFP (MOI-0.001). Kinetics of viral replication was recorded by plaque assay.

6.9 Animal experiments

6.9.1 Ethics statement

All animal experiments were performed according to the guidelines of the German Animal Welfare Law (AZ 33.9-42502-05-12A295 and AZ 33.14.42502-04-070/08). The approved animal code is 070/08 and 11/0528.
All preparative work was carried out under semi-sterile conditions and to avoid contamination with exogenous pathogens, all devices were thoroughly cleaned, disinfected with 70% ethanol and autoclaved.

6.9.2 Animal housing

Transgenic mice are bred and maintained in the tier 1 facility of the Helmholtz Centre for Infection research (HZI) under SPF conditions.C57BL/6 or WT mice were bought from Harlan Laboratories. The genotypes of all mice were verified by PCR.

Before infection, mice are transferred to the tier 2 facility (S2). In both facilities at the HZI, mice are maintained in standard ventilated cages standard (IVC system Green Line, Tecniplast Germany GmbH) in same-sex groups. Standard conditions for housing of animals include twelve-hour light-dark cycle, air exchanges of 15 times per hour, illuminance of 50 lux, temperature of 22 ° C, 55% humidity, water and food pellets.

Table 5: List of Mice used in this study

Genotype	Background	Reference
C57BL/6	C57BL/6	Harlan Laboratories
Thy1.1	C57BL/6	[143]
CD45.1	C57BL/6	[144]
IRF-$1^{-/-}$	C57BL/6	[145]
$IFNAR^{-/-}$	C57BL/6	[146]
IRF-$3^{-/-}$	C57BL/6	[54]
IRF-$7^{-/-}$	C57BL/6	[147]
IFN-$\beta^{+/\Delta\beta\text{-luc}}$	C57BL/6	[112]
MX2luc	C57BL/6	[113]
$IFNAR^{fl/fl}$CreERT	C57BL/6	[108]
$IFNAR^{fl/fl}$$NesCre^{+/-}$	C57BL/6	[108]

6.9.3 Blood isolation and serum collection

Blood could be drawn by two different methods; cardiac puncture and isolation from the retroorbital vein. For the former, mice were killed with CO_2, their chest was cut open and a syringe with a 0.55X25mm needle was used to draw blood from the heart. To draw blood from a living mouse, mouse was firmly ficked by the neck and the retrobulbar venous plexus which is a vein that lies in the corner of the eye was punctured with a glass capillary. Then by applying the right amount of pressure the glass capillary was twisted in till blood flowed out into the capillary.

To obtain the serum, blood was incubated for 2 hours at RT or overnight at 4 ° C to ensure blood coagulation. To separate the serum from the coagulated blood, samples were centrifuged at 2000g for 20 min. The top clear phase was the serum which was then isolated.

6.9.4 Adoptive transfer

After purifying pan T ($CD4^+$ and $CD8^+$ T cells) cells isolated from a congenic mouse by magnetic separation **(refer 6.20)**, 1×10^7 cells were injected i.v into each mouse in 100µl PBS. 48 hours post transfer, success of transfer was

analysed by tracing back the injected cells by flow cytometry **(refer 6.19)**. Mice were subsequently infected with VSV **(refer 6.9.7)**.

6.9.5 Bone marrow chimeras

Bone marrow chimeras were generated with modifications to the previously described protocol [148].

6-8 week old WT and IRF-$1^{-/-}$ mice were irradiated with a lethal dose of 950 rad. The next day bone marrow were isolated from the tibia and femur of 4-6 week old IRF-$1^{-/-}$ or WT (CD45.1) mice and were injected i.v. with 1 $x10^7$ bone marrow cells in 100µl PBS into the irradiated mice. Mice were kept on antibiotics (Baytril) for 2 weeks. Six-eight weeks after bone marrow transplantation, WT (CD45.1)→WT (CD45.2), IRF-$1^{-/-}$ (CD45.2)→WT (CD45.1), WT (CD45.1)→IRF-$1^{-/-}$ were bled via retro-orbital puncture **(refer 6.9.3)** to evaluate the efficiency of chimerism **(table 6)**. The next day chimeric mice were infected i.n with VSV. Survival of chimeras was monitored.

Table 6: Transplantation efficiency in the chimeric mice

	WT → WT	**WT → IRF-$1^{-/-}$**	**IRF-$1^{-/-}$ → WT**
% Donor cells found in the blood of chimeras	85,6	81,6	96,2

6.9.6 Administration of anaesthesia

For short term anaesthesia, 1-2 ml isoflurane (Albrecht) was poured on a tissue and placed in a container. The mouse was placed in the container, covered with the lid and observed until it became unconscious. Mice stay anesthetized for 30 seconds with this procedure.

To administer anaesthesia for longer time periods, mice were injected 100 µl/10 g body weight a sterile solution of 10% ketamine (WDT), 5% Rompun or Xylazin (CP-Pharma) in 0.9% Nacl. This procedure allows mice to stay unconscious for approximately 30 min.

6.9.7 Virus infection

For intranasal infection (i.n), mice were anesthetized with ketamine / Rompun or xylazine solution and thus placed under general anesthesia **(refer 6.9.6)**. All virus infections were carried out with $5X10^6$ pfu of VSV/VSV-eGFP and 0.04 MLD50 of Influenza A virus PR8/A/34unless stated otherwise. Virus was mixed with PBS to a total volume of 20µl and administred carefully into both nostrils.

For intravenous infection (i.v.), virus suspended in 100µl of PBS was administered into the tail vein of the mouse.

6.10 Virus quantification from tissues

Virus titers from tissues were carried out as previously described with minor modifications [108]. In brief, VSV infected mice were euthanized and blood was removed from organs by cardiac perfusion with 25 ml of PBS. Organs were isolated and were snap-frozen in liquid nitrogen. On the day of the experiment, organs were thawed, weighed; homogenized using Fast Prep 24 (MP) in 1.5 ml of PBS. The homogenised organ mixture was centrifuged at 2000g for 30 min and 200µl of the supernatant was used to quantify the total amount of virus in 10-fold serial dilutions on Vero cells by plaque assay. Results are expressed as plaque-forming units (pfu) per gram of tissue.

6.11 IFN-α ELISA

The amount of murine IFN-αs in mouse serum was determined by enzyme-linked immunosorbent assay (ELISA) according to the manufacturer's instructions (eBioscience).

6.12 In vivo imaging

For *in vivo* imaging, mice were injected intravenously with 150 mg/kg of D-luciferin in PBS (CaliperLS), anesthetized using Isoflurane (Baxter) and monitored using an IVIS 200 imaging system (CaliperLS). Photon flux was quantified using the Living Image 3.2 software (CaliperLS).

6.13 Determination of viral titres/ Plaque assay

For the detection and quantitation of infectious viral particles, plaque assay was performed. Since VSV is a cytopathic virus, the virus creates a pattern of holes on a uniform cell layer due to infecting neighbouring cells. These holes are referred to as plaques. To quantitate VSV from organs tissues, they are first homogenized in 1.5 ml of 1% BSA using FastPrep-24 (MP). The sample is centrifuged at 2000g for 30 min. A fraction of the supernatant is collected and added to a confluent layer of VERO cells in a series of 10-fold dilutions and incubated for 2 hours at 37°C.

To quantitate virus from the supernatant of virus infected cells, a fraction of the supernatant is collected and added to a confluent layer of VERO cells in a series of 10-fold dilutions and incubated for 60 min 37°C.

After the incubation of VERO cells with the virus culture, the supernatant was removed and the cells were overlaid with 1:1 mixture of 2 x DMEM with 10%

FCS / 2% (w / v) methyl cellulose (high viscosity) to prevent free movement of the virus in the culture medium. After 2 days, cells were stained with crystal violet (1% crystal violet, 3.6% formaldehyde, 1% methanol, 20% ethanol) and the virus titre was determined by counting the number of plaques.

6.14 Virus Neutralisation Assay

The virus neutralization assay is a variant of plaque assay **(refer 6.13)** where virus specific antibodies can be detected and quantified. The assay works on the principle that virus specific antibodies from the serum bind to the virus and thus neutralize the entry of the virus into the cell. The distinction between IgM and IgG antibodies can be done by the addition of 2-mercaptoethanol which disrupts the IgM structure. This allows the measurement of only VSV specific IgG antibodies. The protocol for quantification of VSV specific IgM and IgG responses were done as described previously [149].

Serum was diluted 1/40 and incubated with or without 2-mercaptoethanol for 1 hour. Treated or non-treated sera were pre-diluted 1:40; heat inactivated at 56°C for 30 min, diluted 40 fold and then diluted 1:2 with 500 pfu/ml VSV. The serum-VSV mixture was incubated for 90 min at 37°C and then transferred onto VERO cells in a series of 2 fold dilutions. After 60 minutes at 37°C, the supernatant was taken off and medium containing 1 % methyl cellulose was added to the cells. Total plaques were counted after the cells were stained with crystal violet. The dilution at which the serum reduced the plaque number by half was noted as the neutralisation titre.

6.15 Isolating RNA from tissues

While working with RNA, it is necessary that we use RNAse free materials to prevent its degradation. TRIzol works by maintaining RNA integrity during tissue homogenization, while at the same time disrupting and breaking down cells and cell components. Homogenised samples in TRIzol were added with chloroform in a ratio of 1:5 and after the centrifugation, separate the solution into aqueous and organic phases. RNA remains only in the aqueous phase. After transferring the aqueous phase, RNA can be recovered by precipitation with isopropyl alcohol. But the DNA and proteins can recover by sequential separation after the removal of aqueous phase. Precipitation with ethanol requires DNA from the interphase, and an additional precipitation with isopropyl alcohol requires proteins from the organic phase. Total RNA extracted by TRIzol Reagent is free from the contamination of protein and DNA. RNA extraction procedure were carried out using the manufacturer's protocol and stored at -80°C. RNA concentration was determined using the NanoDrop determined.

6.16 Quantitative real time PCR (qRT-PCR)

Total cellular RNA was isolated as described above. RNA in a concentration of 1-5µg was added to cDNA ready-to-go first prime tube (GE health care) in the presence of oligo dT (0.5µg/3µL) and incubated at 37°C for 1 hour. The resulting cDNA mixture was diluted 10 times and RT-PCR was carried out to determine induction of IFN stimulated genes relative to a house keeping gene Beta-actin. To carry out the q RT-PCR, QuantiTect SYBR Green PCR Kit (Qiagen) was used. The PCR reaction mix of 20µl included SYBR Green mastermix, 10pmoles forward and reverse primer and 8µl of 1:10 pre-diluted cDNA. As a negative control, water was used. The reaction cycle included 95°C for 15 seconds, 58°C for 20 seconds and 72°C for 30 seconds.

Table 7: List of PCR primers

Gene	orientation	Sequence
β- actin	forward primer	5'-TGG AAT CCT GTG GCA TCC ATG AAA-3'
	reverse primer	5'- TAA AAC GCA GCT CAG TAA CAG TCC G-3'
IFN-β	forward primer	5'- CTTCTCCGTCATCTCCATAGGG-3'
	reverse primer	5'- CACAGCCCTCTCCATCAACT
IRF-1	forward primer	5'- CTC ACC AGG AAC CAG AGG AA-3'
	reverse primer	5'- TGA GTG GTG TAA CTG CTG TGG-3'
Mx2	forward primer	5'- TCA CCA GAG TGC AAG TGA GG-3'
	reverse primer	5'-CAT TCT CCC TCT GCC ACA TT-3'
Rsad2	forward primer	5'- GTC CTG TTT GGT GCC TGA AT-3'
	reverse primer	5'- GCC ACG CTT CAG AAA CAT CT-3'
USP-18	forward primer	5'- AAG GAC CAG ATC ACG GAC AC-3'
	reverse primer	5'- CAT CCT CCA GGG TTT TCA GA-3'
IFIT-2	forward primer	5'- CAC CTT CGG TAT GGC AAC TT-3'
	reverse primer	5'- GCA AGG CCT CAG AAT CAG AC-3'
IFN-γ	forward primer	5'- TGG CTC TGC AGG ATT TTC ATG- 3'
	reverse primer	5'-TCA AGT GGC ATA GAT GTG GAA GAA-3'
IL28R	forward primer	5'- CCC TGT TTC CTG ACA CTC CC-3'
	reverse primer	5'- TCA GAA AAG TCC AGT GCC CG-3'
IL-1ß	forward primer	5'- TCA TTG TGG CTG TGG AGA AG-3'
	reverse primer	5'- TAA TGG GAA CGT CAC ACA CC-3')
TNF-α	forward primer	5'- TGG GAG TAG ACA AGG TAC AAC CC-3'
	reverse primer	5'- CAT CTT CTC AAA ATT CGA CTG ACA A-3')

6.17 Isolation of leukocytes

Table 8: List of required reagents for isolation of leukocytes

Reagent	Constituents
FACS Buffer	PBS, 2% FCS
ACK (Erythrocyte) lysis buffer	0.15 M NH_4Cl, 10 mM $KHCO_3$, 0.1 mM Na_2EDTA, pH7.2-7.4, sterile
Brain digest solution	PBS, 500 µg / ml collagenase, 0.1 µg / ml TLCK, 10 µg / ml DNase I, 10 mM Hepes

6.17.1 from Spleen

Isolated spleen cells were mashed through a 70 micron cell strainer and reconstituted with 2mM PBS-EDTA as a single cell solution. Erythrocytes were lysed with ACK-lysis buffer and washed twice with FACS buffer.

6.17.2 from Brain

Brain leukocytes were quantitated from a protocol previously described [150]. In brief, whole brains were harvested from uninfected or i.n VSV infected mice. Following perfusion, brains were homogenized through a 70micron cell strainer, digested with a collagenase solution (500 µg/ml collagenase D, 0.1 µg/ml trypsin inhibitor TLCK, 10 µg/ml DNase I, 10 mM HEPES in HBSS) for 1 h at room temperature. Cells were separated by centrifugation at 2000g for 20 minutes on a discontinuous 70-to-30% Percoll gradient. Cells were isolated from the interface, subjected to ACK lysis to eliminate the presence of erythrocytes and washed twice with FACS buffer.

6.18 Isolation of Bone marrow cells

Mice were killed with CO_2. Both legs including the tibia and femurs of mice were cut out and skinned. All muscle tissue surrounding the bone was removed and

the bones were sterilised for 30 seconds in ethanol. Hematopoietic cells were flushed out of a bone with PBS using a 2 ml syringe with a 0.55X0.25mm needle. The cells were then subjected to ACK lysis **(refer 6.17)** and washed twice with PBS.

6.19 Flow cytometry

To identify and quantitate individual cells in a given lymphocytic cell mixture isolated from spleen or brain **(refer 6.17)**, cells were stained with appropriate markers and subjected to florescent activated cell sorting (FACS) analysis. Isolated lymphocytes were first incubated with F_c block to prevent unspecific binding of antibodies for 20 minutes. Antibodies with their appropriate dilutions were then added on the cells and kept on ice for 30 min. Samples were washed three times with FACS buffer and then fixed with the Cell fixation and Permeabilisation kit (BD) according to the manufacturer's instructions.

Table 9: List of antibodies used in this study

Antibody	Produced at	Dilution
Fc block	Group of Molecular Immunology, HZI	1:500
Anti-mouse-CD3 FITC	BD Pharmingen	1:300
Anti-mouse-CD4 APC	BD Pharminen	1:400
anti-mouse-CD8 APCCy7	ebioscience	1:300
Anti-mouse-CD45 PerCPCy5.5	ebioscience	1:500
anti- mouse CD11c PECy7	ebioscience	1:200
anti-mouse CD 45.1 APC	eboscience	1:500
Anti-mouse B220 PE	eboscience	1:400
Anti-mouse DX5 APC	eboscience	1:500
anti- mouse CD11b PE	BD Pharmigen	1:1000

6.20 Isolation of pan T cells by MACS

After acquiring a single cell suspension of spleenocytes **(refer 6.17.1),** Pan T cells ($CD4^+$ and $CD8^+$ cells) were purified by the means of negative magnetic selection using pan T Cell Isolation Kit (Miltenyi Biotec GmbH) and the autoMACS (Miltenyi Biotec GmbH) according to manufacturer's instructions.

6.21 Immunofluorescence

Cultured hippocampal neuronal cells prepared on 13mm coverslips were infected with VSV-eGFP (MOI-0.01) **(refer 6.8.10)**, washed one time with PBS. Cells were fixed with cold 4% (w/v) formaldehyde (PFA) in phosphate-buffered saline (PBS) for 20 min, permeabilised with 0.02% (v/v) Triton X-100 for 3 min, and blocked with 1% (w/v) bovine serum albumin (Applichem) and 10% Goat serum (Sigma) in PBS Markers for neurons- NeuN (Millipore), astrocytes– GFAP (Synaptic Systems) were diluted in blocking solution **(table 10)** and added incubated on the fixed cultures or serum for 60 min, followed by secondary antibodies for 45 min. Images were acquired on LSM Carl Zeiss Confocal.

6.22 Immunohistology

Brains were removed after cardiac perfusion with PBS followed by 4% PFA and incubated 24 hours in 4% PFA followed by an incubation in 30% sucrose in 0.1 M phosphate buffer for an additional 24 hours. Subsequently, the brains were frozen in Tissue Tek® Compound at -80°C. 30 µm sagittal slices of the whole brain were cut using a freezing microtome (Frigomobil, Leica, Germany). All staining procedures were performed free floating. Following a 1 hour blocking step at room temperature in PBS containing 1% BSA, 0.2% Triton and 10% goat serum the slices were incubated over night at 4 °C in primary antibody solution

consisting of 10% goat serum and 0.2% Triton in PBS. Secondary anti-mouse or anti-rabbit antibodies conjugated with Cy2, Cy3, or Cy5 (Jackson ImmunoResearch) were incubated 1:500 in PBS for 2 h at room temperature.

Table 10: List of primary antibodies used for immunofluorescence and immunohistology

Primary antibody	Specificity	Produced at	Dilution
Anti-GFAP	Mouse monoclonal	SIGMA	1:500
Anti-GFP	Mouse monoclonal	Millipore	1:800
Anti-GFP	Rabbit polyclonal	Millipore	1:500
Anti-NeuN	Mouse monoclonal	Millipore	1:500
Anti-IBA1	Rabbit polyclonal	Synaptic Systems	1:500

6.23 Statistical analysis

The results of this work are as mean (± standard error (SEM)) specified. The data generated come from at least two independent experiments. Since the sample size are not large enough to always follow a Gaussian normal distribution, statistical analysis of two independent groups were calculated by the non-parametric Mann-Whitney-Wilcoxon test. Asterisks represent statistical significance between two independent groups. * $p<0.05$, ** $p<0.005$, *** $p<0.0005$.

7 APPENDIX

7.1 List of figures

7.2 List of tables

7.3 References

1. Bowie AG, Haga IR (2005) The role of Toll-like receptors in the host response to viruses. Mol Immunol 42: 859-867.
2. Kawai T, Akira S (2006) Innate immune recognition of viral infection. Nat Immunol 7: 131-137.
3. Alexopoulou L, Holt AC, Medzhitov R, Flavell RA (2001) Recognition of double-stranded RNA and activation of NF-kappaB by Toll-like receptor 3. Nature 413: 732-738.
4. Tabeta K, Georgel P, Janssen E, Du X, Hoebe K, et al. (2004) Toll-like receptors 9 and 3 as essential components of innate immune defense against mouse cytomegalovirus infection. Proc Natl Acad Sci U S A 101: 3516-3521.
5. Hewson CA, Jardine A, Edwards MR, Laza-Stanca V, Johnston SL (2005) Toll-like receptor 3 is induced by and mediates antiviral activity against rhinovirus infection of human bronchial epithelial cells. J Virol 79: 12273-12279.
6. Wang T, Town T, Alexopoulou L, Anderson JF, Fikrig E, et al. (2004) Toll-like receptor 3 mediates West Nile virus entry into the brain causing lethal encephalitis. Nat Med 10: 1366-1373.
7. Guillot L, Le Goffic R, Bloch S, Escriou N, Akira S, et al. (2005) Involvement of toll-like receptor 3 in the immune response of lung epithelial cells to double-stranded RNA and influenza A virus. J Biol Chem 280: 5571-5580.
8. Heil F, Hemmi H, Hochrein H, Ampenberger F, Kirschning C, et al. (2004) Species-specific recognition of single-stranded RNA via toll-like receptor 7 and 8. Science 303: 1526-1529.
9. Diebold SS, Kaisho T, Hemmi H, Akira S, Reis e Sousa C (2004) Innate antiviral responses by means of TLR7-mediated recognition of single-stranded RNA. Science 303: 1529-1531.
10. Lund JM, Alexopoulou L, Sato A, Karow M, Adams NC, et al. (2004) Recognition of single-stranded RNA viruses by Toll-like receptor 7. Proc Natl Acad Sci U S A 101: 5598-5603.
11. Lund J, Sato A, Akira S, Medzhitov R, Iwasaki A (2003) Toll-like receptor 9-mediated recognition of Herpes simplex virus-2 by plasmacytoid dendritic cells. J Exp Med 198: 513-520.
12. Sato A, Linehan MM, Iwasaki A (2006) Dual recognition of herpes simplex viruses by TLR2 and TLR9 in dendritic cells. Proc Natl Acad Sci U S A 103: 17343-17348.
13. Krug A, Luker GD, Barchet W, Leib DA, Akira S, et al. (2004) Herpes simplex virus type 1 activates murine natural interferon-producing cells through toll-like receptor 9. Blood 103: 1433-1437.
14. Delale T, Paquin A, Asselin-Paturel C, Dalod M, Brizard G, et al. (2005) MyD88-dependent and -independent murine cytomegalovirus sensing for IFN-alpha release and initiation of immune responses in vivo. J Immunol 175: 6723-6732.

15. Kato H, Takeuchi O, Sato S, Yoneyama M, Yamamoto M, et al. (2006) Differential roles of MDA5 and RIG-I helicases in the recognition of RNA viruses. Nature 441: 101-105.
16. Chang TH, Liao CL, Lin YL (2006) Flavivirus induces interferon-beta gene expression through a pathway involving RIG-I-dependent IRF-3 and PI3K-dependent NF-kappaB activation. Microbes Infect 8: 157-171.
17. Liu P, Jamaluddin M, Li K, Garofalo RP, Casola A, et al. (2007) Retinoic acid-inducible gene I mediates early antiviral response and Toll-like receptor 3 expression in respiratory syncytial virus-infected airway epithelial cells. J Virol 81: 1401-1411.
18. Samanta M, Iwakiri D, Kanda T, Imaizumi T, Takada K (2006) EB virus-encoded RNAs are recognized by RIG-I and activate signaling to induce type I IFN. EMBO J 25: 4207-4214.
19. Gitlin L, Barchet W, Gilfillan S, Cella M, Beutler B, et al. (2006) Essential role of mda-5 in type I IFN responses to polyriboinosinic:polyribocytidylic acid and encephalomyocarditis picornavirus. Proc Natl Acad Sci U S A 103: 8459-8464.
20. Lindenmann J, Burke DC, Isaacs A (1957) Studies on the production, mode of action and properties of interferon. Br J Exp Pathol 38: 551-562.
21. Pestka S, Krause CD, Walter MR (2004) Interferons, interferon-like cytokines, and their receptors. Immunol Rev 202: 8-32.
22. Pestka S, Langer JA, Zoon KC, Samuel CE (1987) Interferons and their actions. Annu Rev Biochem 56: 727-777.
23. Koyama S, Ishii KJ, Coban C, Akira S (2008) Innate immune response to viral infection. Cytokine 43: 336-341.
24. Stetson DB, Medzhitov R (2006) Antiviral defense: interferons and beyond. J Exp Med 203: 1837-1841.
25. Stetson DB, Medzhitov R (2006) Type I interferons in host defense. Immunity 25: 373-381.
26. Kumagai Y, Takeuchi O, Akira S (2008) Pathogen recognition by innate receptors. J Infect Chemother 14: 86-92.
27. Takeuchi O, Akira S (2007) Recognition of viruses by innate immunity. Immunol Rev 220: 214-224.
28. Takeuchi O, Akira S (2008) MDA5/RIG-I and virus recognition. Curr Opin Immunol 20: 17-22.
29. Meager A, Visvalingam K, Dilger P, Bryan D, Wadhwa M (2005) Biological activity of interleukins-28 and -29: comparison with type I interferons. Cytokine 31: 109-118.
30. Dumoutier L, Tounsi A, Michiels T, Sommereyns C, Kotenko SV, et al. (2004) Role of the interleukin (IL)-28 receptor tyrosine residues for antiviral and antiproliferative activity of IL-29/interferon-lambda 1: similarities with type I interferon signaling. J Biol Chem 279: 32269-32274.
31. Kotenko SV, Gallagher G, Baurin VV, Lewis-Antes A, Shen M, et al. (2003) IFN-lambdas mediate antiviral protection through a distinct class II cytokine receptor complex. Nat Immunol 4: 69-77.

32. Sheppard P, Kindsvogel W, Xu W, Henderson K, Schlutsmeyer S, et al. (2003) IL-28, IL-29 and their class II cytokine receptor IL-28R. Nat Immunol 4: 63-68.
33. Taniguchi T, Ogasawara K, Takaoka A, Tanaka N (2001) IRF family of transcription factors as regulators of host defense. Annu Rev Immunol 19: 623-655.
34. Honda K, Taniguchi T (2006) IRFs: master regulators of signalling by Toll-like receptors and cytosolic pattern-recognition receptors. Nat Rev Immunol 6: 644-658.
35. Tamura T, Yanai H, Savitsky D, Taniguchi T (2008) The IRF family transcription factors in immunity and oncogenesis. Annu Rev Immunol 26: 535-584.
36. Miyamoto M, Fujita T, Kimura Y, Maruyama M, Harada H, et al. (1988) Regulated expression of a gene encoding a nuclear factor, IRF-1, that specifically binds to IFN-beta gene regulatory elements. Cell 54: 903-913.
37. Tanaka N, Kawakami T, Taniguchi T (1993) Recognition DNA sequences of interferon regulatory factor 1 (IRF-1) and IRF-2, regulators of cell growth and the interferon system. Mol Cell Biol 13: 4531-4538.
38. Agresti C, Bernardo A, Del Russo N, Marziali G, Battistini A, et al. (1998) Synergistic stimulation of MHC class I and IRF-1 gene expression by IFN-gamma and TNF-alpha in oligodendrocytes. Eur J Neurosci 10: 2975-2983.
39. Kirchhoff S, Koromilas AE, Schaper F, Grashoff M, Sonenberg N, et al. (1995) IRF-1 induced cell growth inhibition and interferon induction requires the activity of the protein kinase PKR. Oncogene 11: 439-445.
40. Reis LF, Harada H, Wolchok JD, Taniguchi T, Vilcek J (1992) Critical role of a common transcription factor, IRF-1, in the regulation of IFN-beta and IFN-inducible genes. EMBO J 11: 185-193.
41. Bachmaier K, Neu N, Pummerer C, Duncan GS, Mak TW, et al. (1997) iNOS expression and nitrotyrosine formation in the myocardium in response to inflammation is controlled by the interferon regulatory transcription factor 1. Circulation 96: 585-591.
42. Stirnweiss A, Ksienzyk A, Klages K, Rand U, Grashoff M, et al. (2010) IFN regulatory factor-1 bypasses IFN-mediated antiviral effects through viperin gene induction. J Immunol 184: 5179-5185.
43. White LC, Wright KL, Felix NJ, Ruffner H, Reis LF, et al. (1996) Regulation of LMP2 and TAP1 genes by IRF-1 explains the paucity of CD8+ T cells in IRF-1-/- mice. Immunity 5: 365-376.
44. Ogasawara K, Hida S, Azimi N, Tagaya Y, Sato T, et al. (1998) Requirement for IRF-1 in the microenvironment supporting development of natural killer cells. Nature 391: 700-703.
45. Kamijo R, Harada H, Matsuyama T, Bosland M, Gerecitano J, et al. (1994) Requirement for transcription factor IRF-1 in NO synthase induction in macrophages. Science 263: 1612-1615.
46. Lohoff M, Ferrick D, Mittrucker HW, Duncan GS, Bischof S, et al. (1997) Interferon regulatory factor-1 is required for a T helper 1 immune response in vivo. Immunity 6: 681-689.

47. Penninger JM, Sirard C, Mittrucker HW, Chidgey A, Kozieradzki I, et al. (1997) The interferon regulatory transcription factor IRF-1 controls positive and negative selection of CD8+ thymocytes. Immunity 7: 243-254.
48. Jeong JY, Kim SJ, Cho HJ, Hong SH, Lee JY, et al. (2013) Influence of type of nocturia and lower urinary tract symptoms on therapeutic outcome in women treated with desmopressin. Korean J Urol 54: 95-99.
49. Harada H, Fujita T, Miyamoto M, Kimura Y, Maruyama M, et al. (1989) Structurally similar but functionally distinct factors, IRF-1 and IRF-2, bind to the same regulatory elements of IFN and IFN-inducible genes. Cell 58: 729-739.
50. Hida S, Tadachi M, Saito T, Taki S (2005) Negative control of basophil expansion by IRF-2 critical for the regulation of Th1/Th2 balance. Blood 106: 2011-2017.
51. Fitzgerald KA, McWhirter SM, Faia KL, Rowe DC, Latz E, et al. (2003) IKKepsilon and TBK1 are essential components of the IRF3 signaling pathway. Nat Immunol 4: 491-496.
52. Sharma S, tenOever BR, Grandvaux N, Zhou GP, Lin R, et al. (2003) Triggering the interferon antiviral response through an IKK-related pathway. Science 300: 1148-1151.
53. Sato M, Tanaka N, Hata N, Oda E, Taniguchi T (1998) Involvement of the IRF family transcription factor IRF-3 in virus-induced activation of the IFN-beta gene. FEBS Lett 425: 112-116.
54. Sato M, Suemori H, Hata N, Asagiri M, Ogasawara K, et al. (2000) Distinct and essential roles of transcription factors IRF-3 and IRF-7 in response to viruses for IFN-alpha/beta gene induction. Immunity 13: 539-548.
55. Noyce RS, Taylor K, Ciechonska M, Collins SE, Duncan R, et al. (2011) Membrane perturbation elicits an IRF3-dependent, interferon-independent antiviral response. J Virol 85: 10926-10931.
56. Collins SE, Noyce RS, Mossman KL (2004) Innate cellular response to virus particle entry requires IRF3 but not virus replication. J Virol 78: 1706-1717.
57. Honma K, Udono H, Kohno T, Yamamoto K, Ogawa A, et al. (2005) Interferon regulatory factor 4 negatively regulates the production of proinflammatory cytokines by macrophages in response to LPS. Proc Natl Acad Sci U S A 102: 16001-16006.
58. Negishi H, Ohba Y, Yanai H, Takaoka A, Honma K, et al. (2005) Negative regulation of Toll-like-receptor signaling by IRF-4. Proc Natl Acad Sci U S A 102: 15989-15994.
59. Honma K, Kimura D, Tominaga N, Miyakoda M, Matsuyama T, et al. (2008) Interferon regulatory factor 4 differentially regulates the production of Th2 cytokines in naive vs. effector/memory CD4+ T cells. Proc Natl Acad Sci U S A 105: 15890-15895.
60. Tominaga N, Ohkusu-Tsukada K, Udono H, Abe R, Matsuyama T, et al. (2003) Development of Th1 and not Th2 immune responses in mice lacking IFN-regulatory factor-4. Int Immunol 15: 1-10.

61. Takaoka A, Yanai H, Kondo S, Duncan G, Negishi H, et al. (2005) Integral role of IRF-5 in the gene induction programme activated by Toll-like receptors. Nature 434: 243-249.
62. Yanai H, Chen HM, Inuzuka T, Kondo S, Mak TW, et al. (2007) Role of IFN regulatory factor 5 transcription factor in antiviral immunity and tumor suppression. Proc Natl Acad Sci U S A 104: 3402-3407.
63. Barnes BJ, Moore PA, Pitha PM (2001) Virus-specific activation of a novel interferon regulatory factor, IRF-5, results in the induction of distinct interferon alpha genes. J Biol Chem 276: 23382-23390.
64. Ingraham CR, Kinoshita A, Kondo S, Yang B, Sajan S, et al. (2006) Abnormal skin, limb and craniofacial morphogenesis in mice deficient for interferon regulatory factor 6 (Irf6). Nat Genet 38: 1335-1340.
65. Richardson RJ, Dixon J, Malhotra S, Hardman MJ, Knowles L, et al. (2006) Irf6 is a key determinant of the keratinocyte proliferation-differentiation switch. Nat Genet 38: 1329-1334.
66. Honda K, Yanai H, Negishi H, Asagiri M, Sato M, et al. (2005) IRF-7 is the master regulator of type-I interferon-dependent immune responses. Nature 434: 772-777.
67. Lazear HM, Lancaster A, Wilkins C, Suthar MS, Huang A, et al. (2013) IRF-3, IRF-5, and IRF-7 coordinately regulate the type I IFN response in myeloid dendritic cells downstream of MAVS signaling. PLoS Pathog 9: e1003118.
68. Zhao J, Kong HJ, Li H, Huang B, Yang M, et al. (2006) IRF-8/interferon (IFN) consensus sequence-binding protein is involved in Toll-like receptor (TLR) signaling and contributes to the cross-talk between TLR and IFN-gamma signaling pathways. J Biol Chem 281: 10073-10080.
69. Tailor P, Tamura T, Kong HJ, Kubota T, Kubota M, et al. (2007) The feedback phase of type I interferon induction in dendritic cells requires interferon regulatory factor 8. Immunity 27: 228-239.
70. Levy DE, Kessler DS, Pine R, Darnell JE, Jr. (1989) Cytoplasmic activation of ISGF3, the positive regulator of interferon-alpha-stimulated transcription, reconstituted in vitro. Genes Dev 3: 1362-1371.
71. Kimura T, Kadokawa Y, Harada H, Matsumoto M, Sato M, et al. (1996) Essential and non-redundant roles of p48 (ISGF3 gamma) and IRF-1 in both type I and type II interferon responses, as revealed by gene targeting studies. Genes Cells 1: 115-124.
72. Qu L, Feng Z, Yamane D, Liang Y, Lanford RE, et al. (2011) Disruption of TLR3 signaling due to cleavage of TRIF by the hepatitis A virus protease-polymerase processing intermediate, 3CD. PLoS Pathog 7: e1002169.
73. Lei X, Sun Z, Liu X, Jin Q, He B, et al. (2011) Cleavage of the adaptor protein TRIF by enterovirus 71 3C inhibits antiviral responses mediated by Toll-like receptor 3. J Virol 85: 8811-8818.
74. Ahmad H, Gubbels R, Ehlers E, Meyer F, Waterbury T, et al. (2011) Kaposi sarcoma-associated herpesvirus degrades cellular Toll-interleukin-1 receptor

domain-containing adaptor-inducing beta-interferon (TRIF). J Biol Chem 286: 7865-7872.
75. Li XD, Sun L, Seth RB, Pineda G, Chen ZJ (2005) Hepatitis C virus protease NS3/4A cleaves mitochondrial antiviral signaling protein off the mitochondria to evade innate immunity. Proc Natl Acad Sci U S A 102: 17717-17722.
76. Yao XD, Rosenthal KL (2011) Herpes simplex virus type 2 virion host shutoff protein suppresses innate dsRNA antiviral pathways in human vaginal epithelial cells. J Gen Virol 92: 1981-1993.
77. Eksioglu EA, Zhu H, Bayouth L, Bess J, Liu HY, et al. (2011) Characterization of HCV interactions with Toll-like receptors and RIG-I in liver cells. PLoS One 6: e21186.
78. Tamura R, Kanda T, Imazeki F, Wu S, Nakamoto S, et al. (2011) Hepatitis C Virus nonstructural 5A protein inhibits lipopolysaccharide-mediated apoptosis of hepatocytes by decreasing expression of Toll-like receptor 4. J Infect Dis 204: 793-801.
79. Overby AK, Popov VL, Niedrig M, Weber F (2010) Tick-borne encephalitis virus delays interferon induction and hides its double-stranded RNA in intracellular membrane vesicles. J Virol 84: 8470-8483.
80. Espada-Murao LA, Morita K (2011) Delayed cytosolic exposure of Japanese encephalitis virus double-stranded RNA impedes interferon activation and enhances viral dissemination in porcine cells. J Virol 85: 6736-6749.
81. Lin W, Kim SS, Yeung E, Kamegaya Y, Blackard JT, et al. (2006) Hepatitis C virus core protein blocks interferon signaling by interaction with the STAT1 SH2 domain. J Virol 80: 9226-9235.
82. Mossman K, Upton C, McFadden G (1995) The myxoma virus-soluble interferon-gamma receptor homolog, M-T7, inhibits interferon-gamma in a species-specific manner. J Biol Chem 270: 3031-3038.
83. Lin RJ, Chang BL, Yu HP, Liao CL, Lin YL (2006) Blocking of interferon-induced Jak-Stat signaling by Japanese encephalitis virus NS5 through a protein tyrosine phosphatase-mediated mechanism. J Virol 80: 5908-5918.
84. Wang N, Dong Q, Li J, Jangra RK, Fan M, et al. (2010) Viral induction of the zinc finger antiviral protein is IRF3-dependent but NF-kappaB-independent. J Biol Chem 285: 6080-6090.
85. Pine R, Decker T, Kessler DS, Levy DE, Darnell JE, Jr. (1990) Purification and cloning of interferon-stimulated gene factor 2 (ISGF2): ISGF2 (IRF-1) can bind to the promoters of both beta interferon- and interferon-stimulated genes but is not a primary transcriptional activator of either. Mol Cell Biol 10: 2448-2457.
86. Dixit E, Boulant S, Zhang Y, Lee AS, Odendall C, et al. (2010) Peroxisomes are signaling platforms for antiviral innate immunity. Cell 141: 668-681.
87. Schoggins JW, Wilson SJ, Panis M, Murphy MY, Jones CT, et al. (2011) A diverse range of gene products are effectors of the type I interferon antiviral response. Nature 472: 481-485.

88. Nandakumar R, Finsterbusch K, Lipps C, Neumann B, Grashoff M, et al. (2013) Hepatitis C Virus Replication in Mouse Cells is Restricted by IFN-Dependent and -Independent Mechanisms. Gastroenterology.
89. Sen GC, Peters GA (2007) Viral stress-inducible genes. Adv Virus Res 70: 233-263.
90. Hermann DM, ElAli A (2012) The abluminal endothelial membrane in neurovascular remodeling in health and disease. Sci Signal 5: re4.
91. Hawkins BT, Davis TP (2005) The blood-brain barrier/neurovascular unit in health and disease. Pharmacol Rev 57: 173-185.
92. Plakhov IV, Arlund EE, Aoki C, Reiss CS (1995) The earliest events in vesicular stomatitis virus infection of the murine olfactory neuroepithelium and entry of the central nervous system. Virology 209: 257-262.
93. Suthar MS, Diamond MS, Gale M, Jr. (2013) West Nile virus infection and immunity. Nat Rev Microbiol 11: 115-128.
94. Liu NQ, Lossinsky AS, Popik W, Li X, Gujuluva C, et al. (2002) Human immunodeficiency virus type 1 enters brain microvascular endothelia by macropinocytosis dependent on lipid rafts and the mitogen-activated protein kinase signaling pathway. J Virol 76: 6689-6700.
95. Gillet JP, Derer P, Tsiang H (1986) Axonal transport of rabies virus in the central nervous system of the rat. J Neuropathol Exp Neurol 45: 619-634.
96. Pachter JS, de Vries HE, Fabry Z (2003) The blood-brain barrier and its role in immune privilege in the central nervous system. J Neuropathol Exp Neurol 62: 593-604.
97. Hanamsagar R, Hanke ML, Kielian T (2012) Toll-like receptor (TLR) and inflammasome actions in the central nervous system. Trends Immunol 33: 333-342.
98. Hart DN, Fabre JW (1981) Demonstration and characterization of Ia-positive dendritic cells in the interstitial connective tissues of rat heart and other tissues, but not brain. J Exp Med 154: 347-361.
99. Perry VH, Hume DA, Gordon S (1985) Immunohistochemical localization of macrophages and microglia in the adult and developing mouse brain. Neuroscience 15: 313-326.
100. Kierdorf K, Erny D, Goldmann T, Sander V, Schulz C, et al. (2013) Microglia emerge from erythromyeloid precursors via Pu.1- and Irf8-dependent pathways. Nat Neurosci 16: 273-280.
101. Hickey WF (2001) Basic principles of immunological surveillance of the normal central nervous system. Glia 36: 118-124.
102. Hanson RP, Rasmussen AF, Jr., Brandly CA, Brown JW (1950) Human infection with the virus of vesicular stomatitis. J Lab Clin Med 36: 754-758.
103. Sabin AB, Olitsky PK (1937) Influence of Host Factors on Neuroinvasiveness of Vesicular Stomatitis Virus : Ii. Effect of Age on the Invasion of the Peripheral and Central Nervous Systems by Virus Injected into the Leg Muscles or the Eye. J Exp Med 66: 35-57.

104. Emerson SU, Wagner RR (1972) Dissociation and reconstitution of the transcriptase and template activities of vesicular stomatitis B and T virions. J Virol 10: 297-309.
105. Hammond C, Helenius A (1994) Folding of VSV G protein: sequential interaction with BiP and calnexin. Science 266: 456-458.
106. Ferran MC, Lucas-Lenard JM (1997) The vesicular stomatitis virus matrix protein inhibits transcription from the human beta interferon promoter. J Virol 71: 371-377.
107. Ahmed M, McKenzie MO, Puckett S, Hojnacki M, Poliquin L, et al. (2003) Ability of the matrix protein of vesicular stomatitis virus to suppress beta interferon gene expression is genetically correlated with the inhibition of host RNA and protein synthesis. J Virol 77: 4646-4657.
108. Detje CN, Meyer T, Schmidt H, Kreuz D, Rose JK, et al. (2009) Local type I IFN receptor signaling protects against virus spread within the central nervous system. J Immunol 182: 2297-2304.
109. Stojdl DF, Lichty BD, tenOever BR, Paterson JM, Power AT, et al. (2003) VSV strains with defects in their ability to shutdown innate immunity are potent systemic anti-cancer agents. Cancer Cell 4: 263-275.
110. Muller U, Steinhoff U, Reis LF, Hemmi S, Pavlovic J, et al. (1994) Functional role of type I and type II interferons in antiviral defense. Science 264: 1918-1921.
111. Fujita T, Kimura Y, Miyamoto M, Barsoumian EL, Taniguchi T (1989) Induction of endogenous IFN-alpha and IFN-beta genes by a regulatory transcription factor, IRF-1. Nature 337: 270-272.
112. Lienenklaus S, Cornitescu M, Zietara N, Lyszkiewicz M, Gekara N, et al. (2009) Novel reporter mouse reveals constitutive and inflammatory expression of IFN-beta in vivo. J Immunol 183: 3229-3236.
113. Pulverer JE, Rand U, Lienenklaus S, Kugel D, Zietara N, et al. (2010) Temporal and spatial resolution of type I and III interferon responses in vivo. J Virol 84: 8626-8638.
114. Haller O, Acklin M, Staeheli P (1987) Influenza virus resistance of wild mice: wild-type and mutant Mx alleles occur at comparable frequencies. J Interferon Res 7: 647-656.
115. Staeheli P, Haller O (1987) Interferon-induced Mx protein: a mediator of cellular resistance to influenza virus. Interferon 8: 1-23.
116. Prinz M, Schmidt H, Mildner A, Knobeloch KP, Hanisch UK, et al. (2008) Distinct and nonredundant in vivo functions of IFNAR on myeloid cells limit autoimmunity in the central nervous system. Immunity 28: 675-686.
117. Taki S, Sato T, Ogasawara K, Fukuda T, Sato M, et al. (1997) Multistage regulation of Th1-type immune responses by the transcription factor IRF-1. Immunity 6: 673-679.
118. Fensterl V, Wetzel JL, Ramachandran S, Ogino T, Stohlman SA, et al. (2012) Interferon-induced Ifit2/ISG54 protects mice from lethal VSV neuropathogenesis. PLoS Pathog 8: e1002712.

119. Donnelly RP, Kotenko SV (2010) Interferon-lambda: a new addition to an old family. J Interferon Cytokine Res 30: 555-564.
120. Sorgeloos F, Kreit M, Hermant P, Lardinois C, Michiels T (2013) Antiviral type I and type III interferon responses in the central nervous system. Viruses 5: 834-857.
121. Ohmori Y, Hamilton TA (1997) IL-4-induced STAT6 suppresses IFN-gamma-stimulated STAT1-dependent transcription in mouse macrophages. J Immunol 159: 5474-5482.
122. Fujita T, Miyamoto M, Kimura Y, Hammer J, Taniguchi T (1989) Involvement of a cis-element that binds an H2TF-1/NF kappa B like factor(s) in the virus-induced interferon-beta gene expression. Nucleic Acids Res 17: 3335-3346.
123. Fujita T, Sakakibara J, Sudo Y, Miyamoto M, Kimura Y, et al. (1988) Evidence for a nuclear factor(s), IRF-1, mediating induction and silencing properties to human IFN-beta gene regulatory elements. EMBO J 7: 3397-3405.
124. Trilling M, Le VT, Zimmermann A, Ludwig H, Pfeffer K, et al. (2009) Gamma interferon-induced interferon regulatory factor 1-dependent antiviral response inhibits vaccinia virus replication in mouse but not human fibroblasts. J Virol 83: 3684-3695.
125. Ramsauer K, Farlik M, Zupkovitz G, Seiser C, Kroger A, et al. (2007) Distinct modes of action applied by transcription factors STAT1 and IRF1 to initiate transcription of the IFN-gamma-inducible gbp2 gene. Proc Natl Acad Sci U S A 104: 2849-2854.
126. Ramos HJ, Lanteri MC, Blahnik G, Negash A, Suthar MS, et al. (2012) IL-1beta signaling promotes CNS-intrinsic immune control of West Nile virus infection. PLoS Pathog 8: e1003039.
127. Cho H, Proll SC, Szretter KJ, Katze MG, Gale M, Jr., et al. (2013) Differential innate immune response programs in neuronal subtypes determine susceptibility to infection in the brain by positive-stranded RNA viruses. Nat Med 19: 458-464.
128. Chesler DA, Dodard C, Lee GY, Levy DE, Reiss CS (2004) Interferon-gamma-induced inhibition of neuronal vesicular stomatitis virus infection is STAT1 dependent. J Neurovirol 10: 57-63.
129. Chauhan VS, Furr SR, Sterka DG, Jr., Nelson DA, Moerdyk-Schauwecker M, et al. (2010) Vesicular stomatitis virus infects resident cells of the central nervous system and induces replication-dependent inflammatory responses. Virology 400: 187-196.
130. Brundler MA, Aichele P, Bachmann M, Kitamura D, Rajewsky K, et al. (1996) Immunity to viruses in B cell-deficient mice: influence of antibodies on virus persistence and on T cell memory. Eur J Immunol 26: 2257-2262.
131. Fung-Leung WP, Schilham MW, Rahemtulla A, Kundig TM, Vollenweider M, et al. (1991) CD8 is needed for development of cytotoxic T cells but not helper T cells. Cell 65: 443-449.

132. Brien JD, Daffis S, Lazear HM, Cho H, Suthar MS, et al. (2011) Interferon regulatory factor-1 (IRF-1) shapes both innate and CD8(+) T cell immune responses against West Nile virus infection. PLoS Pathog 7: e1002230.
133. Lohoff M, Duncan GS, Ferrick D, Mittrucker HW, Bischof S, et al. (2000) Deficiency in the transcription factor interferon regulatory factor (IRF)-2 leads to severely compromised development of natural killer and T helper type 1 cells. J Exp Med 192: 325-336.
134. Kimura T, Nakayama K, Penninger J, Kitagawa M, Harada H, et al. (1994) Involvement of the IRF-1 transcription factor in antiviral responses to interferons. Science 264: 1921-1924.
135. Dutia BM, Allen DJ, Dyson H, Nash AA (1999) Type I interferons and IRF-1 play a critical role in the control of a gammaherpesvirus infection. Virology 261: 173-179.
136. Reis LF, Ruffner H, Stark G, Aguet M, Weissmann C (1994) Mice devoid of interferon regulatory factor 1 (IRF-1) show normal expression of type I interferon genes. EMBO J 13: 4798-4806.
137. Prinz M, Knobeloch KP (2012) Type I interferons as ambiguous modulators of chronic inflammation in the central nervous system. Front Immunol 3: 67.
138. Suthar MS, Ma DY, Thomas S, Lund JM, Zhang N, et al. (2010) IPS-1 is essential for the control of West Nile virus infection and immunity. PLoS Pathog 6: e1000757.
139. Flodstrom M, Eizirik DL (1997) Interferon-gamma-induced interferon regulatory factor-1 (IRF-1) expression in rodent and human islet cells precedes nitric oxide production. Endocrinology 138: 2747-2753.
140. Fujita T, Reis LF, Watanabe N, Kimura Y, Taniguchi T, et al. (1989) Induction of the transcription factor IRF-1 and interferon-beta mRNAs by cytokines and activators of second-messenger pathways. Proc Natl Acad Sci U S A 86: 9936-9940.
141. Schmitz F, Heit A, Guggemoos S, Krug A, Mages J, et al. (2007) Interferon-regulatory-factor 1 controls Toll-like receptor 9-mediated IFN-beta production in myeloid dendritic cells. Eur J Immunol 37: 315-327.
142. Negishi H, Fujita Y, Yanai H, Sakaguchi S, Ouyang X, et al. (2006) Evidence for licensing of IFN-gamma-induced IFN regulatory factor 1 transcription factor by MyD88 in Toll-like receptor-dependent gene induction program. Proc Natl Acad Sci U S A 103: 15136-15141.
143. Fabien N, Bergerot I, Maguer-Satta V, Orgiazzi J, Thivolet C (1995) Pancreatic lymph nodes are early targets of T cells during adoptive transfer of diabetes in NOD mice. J Autoimmun 8: 323-334.
144. David CS, Shreffler DC, Frelinger JA (1973) New lymphocyte antigen system (Lna) controlled by the Ir region of the mouse H-2 complex. Proc Natl Acad Sci U S A 70: 2509-2514.
145. Matsuyama T, Kimura T, Kitagawa M, Pfeffer K, Kawakami T, et al. (1993) Targeted disruption of IRF-1 or IRF-2 results in abnormal type I IFN gene induction and aberrant lymphocyte development. Cell 75: 83-97.

146. Hwang SY, Hertzog PJ, Holland KA, Sumarsono SH, Tymms MJ, et al. (1995) A null mutation in the gene encoding a type I interferon receptor component eliminates antiproliferative and antiviral responses to interferons alpha and beta and alters macrophage responses. Proc Natl Acad Sci U S A 92: 11284-11288.
147. Daffis S, Samuel MA, Suthar MS, Keller BC, Gale M, Jr., et al. (2008) Interferon regulatory factor IRF-7 induces the antiviral alpha interferon response and protects against lethal West Nile virus infection. J Virol 82: 8465-8475.
148. Schluter D, Kwok LY, Lutjen S, Soltek S, Hoffmann S, et al. (2003) Both lymphotoxin-alpha and TNF are crucial for control of Toxoplasma gondii in the central nervous system. J Immunol 170: 6172-6182.
149. Charan S, Zinkernagel RM (1986) Antibody mediated suppression of secondary IgM response in nude mice against vesicular stomatitis virus. J Immunol 136: 3057-3061.
150. Szretter KJ, Samuel MA, Gilfillan S, Fuchs A, Colonna M, et al. (2009) The immune adaptor molecule SARM modulates tumor necrosis factor alpha production and microglia activation in the brainstem and restricts West Nile Virus pathogenesis. J Virol 83: 9329-9338.

8 ACKNOWLEDGEMENTS

I would like to sincerely thank my supervisor Dr. Andrea Kröger for her supervision and guidance. I would like to thank Dr. Hansjörg Hauser for his critical reason of data and guidance. I would also like to thank Mario Köster for being a part of the intense discussions in our weekly clubs as well as his expertise with confocal microscopy. I would like to express my gratitude to our collaboration partners Martin Korte, Kristin Michaelson-Preusse and Diane Mundil at the Technical University of Braunschweig for their willingness to help me with neuronal culture preparations, confocal microscopy as well as giving us valuable insights to the interpretation of the data generated. I would like to thank Prof. Thomas Schulz and Prof. Dunja Bruder for being a part of my thesis committee. I am also grateful to PD. Dr. Gerhard Gross for willing to be my mentor at the TU. My sincere gratitude to Ms. Martina Grasshof for her excellent technical expertise. A special thanks to Dr Bishnudeo Roy for helping me with technical procedures and his “post-doc” advice. My appreciation to Dr. Sabine Kirchoff, Daniela Romke and the rest of the HZI graduate school team for being an outstanding support to graduate students. I would like to thank my labmates Katja and Ramya for everything they have done. I would also like to thank the EXIL group Danim, Haanas, Lucas and Markus for being excellent colleagues. I would like to thank Bushra, Vinay, Upneet and Shawal for being such dependable friends.

I would like to thank my friends and family from India for being so supportive and patient with me. My heartfelt thanks to Matt Wilson for being so supportive, encouraging and amazing to me.